We would like to thank the reviewers for the insightful and helpful comments and suggestions. The response to each comment is below in italics.

RESPONSE TO REVIEWER 1

The paper describes one of the instruments now making regular measurements of tropospheric ozone at a high-altitude, sub-tropical Southern Hemisphere observatory on Reunion Island in the Southern Indian Ocean. The location of the observatory is in a region of the globe that is under-represented in regular atmospheric observations. The paper is written to demonstrate the quality of the measurements and, as such, there importance in adding to the understanding of global ozone concentrations. The paper provides a chronology of measurements on the island and describes the advantages of the mountain site over the previous sea level site. It is well written and deserving of publication.

Page 2. Several sites are discussed here, Gillot, near the coast, where sondes are launched; the Université de la Reunion, where a lidar was first installed, and the Maido site. It would be helpful to have a small Table here with the Lat., Lon., Altitude and distances between the sites. It puts the information in a single location. In the related Figure 1, the color scheme makes some of the print difficult to read – this may be exacerbated in the printing process.

Figure 1 is changed and Table 1 gives the coordinates and altitudes of the measurements sites as well as their distance from the Maïdo Observatory.

Pages 3 and 5. In the discussion of the Raman cell it is not clear if the laser beam is focused into the cell or not. My reading of this (and Figure 5) would lead me to believe that it is not, but this should be stated if it is the case. Also some information as to why such a choice was made. What is the efficiency of the conversion into each of the Stokes lines? D2 pressure in the cell? Here too, a small table with the input and output parameters of the Raman cells for each of the two systems is helpful in understanding any differences noted in the measurements.

The LIO3T and LIO3TUR rely on the same design. The Raman cell is equipped with two silica window lenses that had a focal distance of 75 cm to focus the beam as closely as possible to the center of the cell for optimal stimulated Raman scattering. Details regarding this Raman cell as well as the efficiency of the conversion into each of the Stokes lines are stated in Baray et al. (1999). We do not state this in the article as it is detailed in previous published papers.

Page 4, Line 27: “decrease” should be “decreases”

Done.

Page 5, Line 14: It states that a Hamamatsu 9980-110 PMT is used. I could not find a datasheet for a -110 variant of the R9980. Should this be an R9880-110? The quantum efficiency of the R9980 is quite low below 300 nm, whereas the R9880 is significantly higher. If this is a 9880-110 is it used at

the 289 wavelength? This tube is susceptible to signal induced noise in the UV. The R7400 has much better characteristics than the 9880-110 at these wavelengths, but it has less gain.

This is correct: this is a R9880-110 (not a R9980-110) and it is used for the 289nm channel. It is corrected page 6 line 7. R7400 could indeed be used with benefits for the 289nm detection channel, and, following your comments, this is something we plan to do in a near future.

Page 6, Line 26: should this end "with an uncertainty of 5%."?

Corrected.

Page 7, Line 19: Mount should be Observatory

Corrected.

Page 7, Line 23: Delete "Laser and Raman Cell", insert "at the transmitted wavelengths,"

Corrected.

Figures 6,7 – Is the fact that there are increasing vertical resolutions as the integration time increases (Figure 6), responsible for the higher uncertainty for the one hour integration, compared with the 20 minute integration?

Uncertainty increases when integration time decreases because of the increasing detection noise (i.e. decreasing signal to noise ratio).

How are the vertical resolutions determined? Is a maximum desired uncertainty used to select the vertical resolution?

Vertical resolution is not selected through a uncertainty threshold, but is calculated as described in Section 2.2.

Figure 8: There is a discontinuity seen at 14 km in both panels. Is this also due to some measurements not reaching beyond this altitude? Was this sonde or lidar related? Figure 9 shows remnants of the same discontinuity.

The "discontinuities" in the mean profiles shown on Figure 8 and 9 are caused by the varying valid ranges in the LIO3T profiles. It is stated page 8 lines 7 and 33. Moreover, Figures 5 and 6 now show the number of LIO3T profiles with respect to the altitude.

Page 8, Lines 24 – 28: Was there a reason for using the non-standard solutions in the sondes at Gillot? If so this should be stated.

The use of a non standard solution was a mistake.

Page 9, Line 5: Insert “The” before “valid range”.

Corrected.

Page 9, Line 7: delete “until”, insert “near”

Corrected.

Page 9, 14-19. If a Morgane campaign curtain plot of the lidar retrieved aerosol scattering ratio is available, this would be a good place to insert that to go along with the discussion of the volcanic plume. At what altitude were the stratospheric intrusions located. Is this enhanced aerosol visible in the daily ASR plots? This should show up in the figure mentioned here.

Enhanced aerosol loadings (likely coming from the Calbuco eruptions) were observed with the 532nm backscattered signal of the LIO3T (not shown) in these stratospheric air masses entering the troposphere above Reunion Island, which could have disturbed the ozone detection and quantification by the LIO3T, and consequently lower the agreement between LIO3T and ECC soundings during this period. These stratosphere-to-troposphere exchanges involving a volcanic plume above Reunion Island will be the subject of a dedicated study. This is now stated page 8 line 24-28.

Page 10, Line 19: “co-located” should be changed to “compared”

Corrected.

Page 10, Line 23: “set a comparable” should be “set of comparable”

Corrected.

Page 12, Line 9: delete “to a NDACC labellisation” insert “for inclusion within NDACC"

Corrected.

RESPONSE TO REVIEWER 2

General Comments:

It should be reiterated throughout the text which lidar system (old vs. new) is being described. Although the subscript "_UR" is used to denote the old system, I still found several instances confusing as to which lidar data was presented.

The structure of the article is changed to make it clearer along the text.

Figure 1: Recommend adding ECC, LIO3T, and LIO3t_UR to the map after site location. Also altitude site altitude would be helpful.

Figure 1 now indicates were the used instruments are located. Table 1 gives coordinates and altitude of the sites.

Figure 2: The VR and uncertainty are effectively presented in Figure 6/7 for the new instrument. The information in Figure 2 could be simply stated in the text at various altitudes or added as a component to complement figure 6/7. Or conversely, bring in the new lidar VR/Uncertainty budget here as well to simultaneously show the absolute uncertainty as well as improvement to the system.

VR and uncertainties are now provided for both systems on Figures 3 and 4, respectively.

Figure 3: It would be useful to add the occurrences (with a different color) for the new system. It is stated later in the text and elaborated in Figure 14, but may make more sense to have towards the beginning to complement the old lidar system. Conversely, you could move all of the lidar/ECC discussion to the end (where Figure 14 currently exists).

The article outline is modified and the ECC, LIO3TUR and LIO3T climatologies are given and discussed Section 5. Moreover, Figure 10 is now more consistent with Figure 11 and gives the monthly distribution of the number of profiles for ECC, LIO3TUR and LIO3T.

Section 2.2 and Figure 4: Does the missing data (e.g. December above 10 km) in bottom panel Figure 4 correspond to lack of lidar coverage? Or the uncertainty of the measurement was larger than a certain threshold?

We have only one December profile measured by LIO3T for the 01/2013-01/2016 period, and this profile ends up at 10km due to a misalignement of the lidar. It is stated page 11 lines 5-6.

It would be helpful to recreate the occurrences in Figure 3 as the same layout as Figure 4 but monthly instead of yearly.

Figure 10 is now more consistent with Figure 11 and gives the monthly distribution of the number of profiles for ECC, LIO3TUR and LIO3T.

Generally the ECC shows higher ozone between 10-16 kms, regardless of time of year. Is this a known issue? Relevant to sonde reprocessing?

The ECC climatology is now done with the reprocessed ECC database (Witte et al., 2017) and with a correction applied to take into account the non-standard ECC/solution pairing (cf. Section 4.1). As a result, these greater ozone concentrations between 10-16km previously pointed out by ECC do not appear anymore.

and more importantly, are these differences within the uncertainty of the lidar measurement (with a set vertical resolution/temporal averaging)? A difference plot may highlight potential differences.

The goal of this paper is not to validate LIO3TUR measurements, and ECC and LIO3T measurements are compared (for LIO3T validation) in Section 4.1 for both Gillot and Maïdo soundings with a better accuracy in the comparison than the one that would be obtained from a plot of the difference between two climatologies.

Is the ECC climatology only from Gillot or combination of Gillot/Maido?

Figure 11 only shows Gillot climatology.

Figure 6: Are the differences observed between 6-8 km geophysical or based on the algorithm/processing? Is there a sounding for this observational period to compare with? I would assume the SNR to be largest from 6-8 kms and therefore the temporal averaging would generate less obvious differences. Is it possible there is a partial overlap or saturation correction that needs to be addressed?

The differences are geophysical and unfortunately no sounding is available during the period. Anyway, we decided to remove this figure as it does not bring any information with respect to the scope of this article, which is not to analyse any case study.

L25 – Remove “5The”

Corrected.

Figure 7: Are these uncertainties explicitly based on the retrievals performed in Figure 7 or are these average uncertainties over many nights. It seems odd that at 8 kms, there is a greater uncertainty from a 1 hr measurement than at 20 mins. Please clarify.

These uncertainties are for the entire dataset. There was a mistake in the uncertainty calculation, due to the various valid ranges troughout the dataset. This is now corrected (Figure 4).

P8L23 – Is Witte et al., still in prep or under review?

Witte et al. is now in review. It is corrected page 7 line 24 and in the references.

P9L9 – Should be McGee, not MacGee

Corrected.

Figure 8/9: There appears to be the largest difference between the lidar and ECC below 8 kms. Is this systematic for all 8 launches? Is this also apparent in the original lidar data?

No, this not systematic for the 8 launches.

Were these sondes launched from Gillot or Maido?

Figure 5 shows comparison between LIO3T and ECC sondes launched from Maïdo, and Figure 6 between LIO3T and ECC sondes launched from Gillot.

It is useful to have a profile of the number of comparisons to make discontinuities apparent.

Right. Figures 5 and 6 now give the profile of the number of comparisons.

If the potentially contaminated (e.g from aerosols) data were removed would the results improve?

We did not make the exercise yet, but the use of the 532nm channel to detect and possibly discard aerosol layers from ozone retrieval is in our future plans.

Eq 6, what is reference for the 200 in the numerator? Is this based on sample size?

The 200 comes from the fact that we use the relative difference between two observations ("r"), using the mean value of these 2 observations to not considere anyone as the reference one. Equation 6 is now made more explicit.

Figure 11: What's driving the difference in FTIR uncertainty from the beginning of the time series to the end? Is this the full uncertainty or partial uncertainty? Bottom panel ylabel can just be D.

The full uncertainty is used here for the FTIR and the lower uncertainty shown in 2013 was a mistake. It is now corrected.

Further suggestion #1: Instead of the cross histogram in figure 15, show a complete time series of all the data in the archive used to make this plot. Showing the reader the entire data set instead of the histogram will emphasize the observed variability in O3.

This is a good suggestion. However, we chose not to present the LIO3T time serie because it is too sparse for the time being (84 profiles over 1084 days) to make it easily readible.

Further suggestion #2: One very unique piece of information at the lidar site location is the ability to observe this enhanced O3 related to biomass burning. In the section describing the IASA comparisons, it may be helpful to show a world map of one day (or gridded month) where Maido is directly in the center of a CO transport plume, therefore highlighting the location and detection capabilities of the instruments.

The interesting location of the site to observe biomass burning plumes is already documented in numerous previous studies using with ground-based (e.g. FTIR, lidar, ECC) and satellite (e.g. IASI, CALIPSO, MODIS) observations. Consequently, we do not think it is necessary to include such a world map in this paper.

RESPONSE TO REVIEWER 3

General comments :
This paper is indeed well in the scope of the journal, but needs to be improved before acceptance. The manuscript appears as not enough mature, missing frequently of accuracy with lack of definitions and arguments. Provide sections 3.2.1, 3.2.2 and 3.2.3 earlier in the manuscript because these informations should be available for the lidar when operated at l'Université de la Réunion.

Sections 3.2.1, 3.2.2 and 3.2.3 are now provided earlier in the manuscript.

Equation 6, correlated text and figures are unclear and I will not address any comments there, unfortunately a key point in your study. Improve Figures and to suppress the figures or table when not enough informative and avoid repetitions. Material should be valuable with a real effort and some work to reinforce the demonstration and the benefits/limits from this new instrumentation.

Equation 6 is now clarified and "not-usefull-enough" Figures and Tables are removed.

Specific comments (not extensive) :
Title should be revised discarding Part 1 which is not meaningful. I suggest : « Ozone profiles from a DIAL lidar at Maïdo Observatory (Reunion Island): instrumental description, instrumental performance, and result comparison with ozone external data set. »

This suggestion is taken into account in the new title. However, "Part 1" is kept because this paper is the companion article of an upcoming one dealing with stratospheric ozone measurements in Reunion Island, which will be the "Part 2".

Your paper is based on a DIAL instrument...but DIAL is nowhere defined as a Differencial Absorption Lidar. Please define this acronym at least once.

The DIAL acronym is now defined in the abstract and in Section 2.1.

This lidar technique is now well known and you refer to major technical points already published regarding your instrument (ex line 31 p3-line 1 p4) and data processing. Highlight what is new regarding LIO3T instrument and performance as compared to previous published papers.

This work mainly aims to validate the LIO3T measurements. As, indeed, technical description of the instrument can be found in previous published papers, we now refer to these previous papers and only state the most important features of the system.

Please discuss the uncertainty from your figure 2 versus figure 7 and explain why the results are similar/different with respect to altitude.

There was a mistake in the uncertainty calculation due to the various valid ranges troughout the

lidars datasets. It is now corrected and results are more consistant.

Homogenize your instrument labelling. Fix it once and make it consistent all along the text, including abstract, figures and tables. Along the text, you used : ozone lidar system (LIO3TUR), LIO3T, LIO3T O3, LIO3TUR, system, current system, current LIO3T system, LIO3T system, LIO3T lidar, LIO3T low and LIO3T high (this two latest are undefined elsewhere and used also in the abstract - unclear). For example I suggest to replace sentence starting line 10 page 3 by : "In the following, the lidar installed at the Université de la Réunion will be referred as LIO3TUR whereas the one installed at the Maïdo Observatory will be referred as LIO3T". Two labelling seems enough. If you need more, clearly explain.

Instrument labelling is now consistent. However, we did not change line 10 page 3 because we do not want the reader to believe that both system (LIO3TUR and LIO3T) are currently operating (only the LIO3T – at the Maïdo Observatory – operates). Regarding the "LIO3T low" and "LIO3T high", they are not labels, they indicate if LIO3T is in average higher or lower than the ancillary dataset. It is now made more explicit.

Revise and Clarify line 5 p2 : "Ozone is a major greenhouse gas in the upper troposphere and lower stratosphere". Insist on radiative forcing contribution and remove "major"...
Rephrase lines 14-15 p2 and justify "great interest" to document climate change.
Line 20 p2 : "To improve the operation of remote sensing instrument" remote sensing is imprecise. Do you refer to space-borne instrumentation?... and operation seems not appropriated. Replace "a 2160m-high atmospheric facility" by "a high atmospheric facility" to avoid repetition. You provide afterwards geographical coordinates and altitude.

Introduction is now revised and clarified with respect to these comments.

Figure 1 : Gillot in black is difficult to see and altitude would be here welcome (figure already published please provide reference).

Figure 1 is changed and coordinates (including altitudes) are given for each site on Table 1.

Additional general comment on altitude: mention once all altitudes in your manuscript will be provided in amsl and avoid to repeat latter.

Done on page 6 line 14.

Replace title section 2 by "Historical context of the lidar installed at the Université de la Réunion (LIO3TUR, 1998-2010)

The article outline is changed and we now describe the LIO3TUR and LIO3T in the same Section (3.1).

Replace title section 2.1 by “Instrumental description” or “Instrumental characteristics”

Done.

Line 7 p4 : First sentence is really too short...Is that your result? Could you explain the altitude range limitation? Don’t forget your goal Line24 p3 is to provide data "over the entire tropospheric column...".

This range validity is now justified by the overlap factor and signal-to-ratio (page 6 lines 13-14). Moreover, the “over the entire tropospheric column” sentence is now removed and replaced by “In 1998, an extension was installed to the existing system to perform ozone measurements in the free troposphere, including the upper troposphere” (page 5 line 22).

Figure 2 : by “resolution” you mean “vertical resolution”...

Yes, X label is now clarified.

What is the criteria for uncertainty? It is defined lately for LIO3T.

The same criteria apply for the LIO3TUR uncertainty and the Data processing sections are now provided before.

It would be valuable in addition to have uncertainty expressed with the ozone unit provided. Explain why such a change in the uncertainty of LIO3TUR with respect to altitude. Please modify your X-axis (top and bottom) giving a more precise scaling (more minor ticks).

Done.

Line 9 p4 : “Temporal resolution... was chosen depending on atmospheric conditions”...Please justify what is your criteria.

The atmospheric conditions mentioned here are the cloud free sky duration. It is now clarified in the text (page 6 line 16).

Figure 3 and Figure 4 : please provide consistent figures. The number of profiles given per year is non adapted and consistent to support a monthly-averaged climatology. Note than < 10 profile per year is extremely low. Provide the monthly statistics for the ECC sondes, the LIO3TUR and LIO3T in a panel of your figure 4 , deep gaps within years could be specified in the text and you might suppress figure 3. Please replace figure 4 caption by “Monthly O3 climatology derived from ECC sondes over 2005-2015 at Gillot site between 0 and 19km (Top left panel), from LIO3TUR over 1998-2010 at Université de la Réunion campus site between X and XXkm (Top right panel) and from LIO3T over 2013-2015 at Maïdo Observatory between X and XXkm (Bottom panel).”.

Figure 10 now shows the monthly statistics for ECC, LIO3TUR and LIO3T and Figure 11 caption is

changed.

Comparing the ECC sondes and LIO3TUR climatology, your figure 4 points out within 10-16km greater ozone concentrations from the ECC sondes...Explain, please.

The ECC climatology is now done with the reprocessed ECC database (Witte et al., 2017) and with a correction applied to take into account the non-standard ECC/solution pairing (cf. Section 4.1). As a result, these greater ozone concentrations between 10-16km previously pointed out by ECC do not appear anymore.

Replace title section 3 by "The lidar installed at the Maïdo Observatory (LIO3T, 2013-present)"

As LIO3TUR and LIO3T are now presented in the same Section (3.1), this section does not exist anymore.

Line 31 p4 : "Many instrument" is very imprecise.

The sentence is changed.

Line 32 p4 : "another lidar" is imprecise. Which one : the LI1200 ?

Right. It is now clarified in the text.

Replace 3.1 in title "current system". In this paragraph, a similar description has been provided in Baray et al. (2013) and citation is missing. Is there something new?

Yes, description of the system can be found in Baray et al. (2013) and there is nothing new on this system since 2013. We now only state the main important features of the system.

Suppress lines 18-20 from this paragraph, probably the right place would be in "conclusions and future plans".

Done.

Please consider Table 1 and Figure 5 and try to avoid repetition between both. Table 1 should be probably suppressed.

This is right ; Table 1 is suppressed.

Please modify in Figure 5 caption using "LIO3T instrumental schema" ... I expect you are referring

here precisely to LIO3T at Maïdo Observatory???

Figure 2 caption is modified, and yes, we are refering to the LIO3T (at Maïdo Observatory).

Line 23 p5 : “two backscattered lidar signal at two different wavelength” Check if correct.

It is correct.

Line 24 p5 : be more concise. I suggest “...wavelength, at 289nm (lon) where ozone is strongly absorbed and at 316nm (loff) where ozone absorption is weaker”.

This sentence is now more concise.

Line 28 p5 to Line 7 p6 : please avoid repetitions. Fix once z as the altitude and l as the wavelength. Please provide the interfering gas.

Repetitions are now avoided. Regarding the interfering gases, according to Leblanc et al. (2016), the interfering gases to consider in practice are NO2, SO2, and O2. NO2 and SO2 are negligible in most cases of tropospheric ozone retrieval, except in heavy volcanic aerosols loading conditions. The absorption by O2 should be considered if any of the detection wavelength is shorter than 294nm (which is the case here as we use the 289nm wavelength). However, in our case, we do not take into account any interfering gases for the time being. It is part of our future plans to include them in the “DIAL” code. This is now stated page 4 lines 3-8.

Line 7 p6 : This last sentence introduces further 3.2.2, specify. Additionally replace “this” by the equation number to be precise.-

Done.

Replace 3.2.2 title I suggest to replace by Saturation, correction and consequences on the vertical resolution

Done.

Line 9 p6 : “Saturation” what is saturated and what is the cause and why below 7km.

The saturation is defined as a difference between the number of photons received by the detector and the number of photons acquired. It is a non-linear phenomenon, depending on the dead time of the detector. In the LIO3T case, due to the detector sensitivity and the geometry of the instrument, we found that saturation occurs only below 7km. This is now clarified page 4 lines 10 and 16.

Line 13 p6 : ‘etc’. Rephrase the sentence”...type of filter such as....

Done.

Line 14 p6 : replace “described” by extensively detailed.

Done.

Line 15-16 p6 : “we decide”...replace by we found and rephrase but add (not shown)

Done.

Line 18 p6 : “the resolution rises” Modify expression. Compare the vertical resolution to figure 2 and explain.

The sentence is corrected and the vertical resolutions are presented in Figure 3 and Section 3.2.

Figure 6 : Modify the resolution lines using dashed lines and modify caption on the figure in order to discriminate ozone profiles and the vertical resolution given with respect to integration time. In the figure caption, origin of data (LIO3T) is missing.

Figure 6 is suppressed it does not bring any information with respect to the scope of this article, which is not to analyse any case study.

Line 26 p6 : Please check here “to 5The”

Done.

Line 9-10 p7 : “new tropospheric ozone version...” the details on cross-sections and uncertainty you provide is not much informative and information seems different from line 25-26 p6.

This sentence is suppressed (not very usefull indeed).

Line 11-17 p7 : not at the right place, better place could be in conclusions and future plans

Done.

Line 25-26 p7 : explain why only at night.

Done page 6 line 13.

Explain why such integration time changes with respect to the data you compare to.

Done page 6 line 27 and page 8 line 6.

Line 28-30 p7. Please rephrase this sentence. “Notably” is imprecise, how much and where, but note the consistency within ~9-11,5km and explain.

We removed this figure as it does not bring any information with respect to the scope of this article, which is not to analyse any case study.

Line 4 p8 : “goes” replace by varies

Done.

Figure 7 : Why LIO3TUR uncertainty increases by a factor of 3 at least above 13km whilst the one of LIO3T decreases above 14km whatever the integration time by a factor of 2 at least.

There was a mistake in the uncertainty calculation due to the various valid ranges troughout the lidars datasets. It is now corrected and results are more consistant.

Revise section 4 title. Comparison is really too short here. What pieces are you comparing.

Section 4 title is now “Comparisons with ancillary data”.

Line 9 p8 ‘validate’ Do you compare, evaluate or validate?...Keep constant and take care when using validation concept. I would say here you evaluate...

One of the main goals of this paper is to validate the LIO3T measurements by comparing them to ECC soundings (which are commonly used for this purpose). We consider that this work is a validation of the LIO3T measurements.

Line 13p 8 add IASI after space-borne and replace instrument by data.

Done.

Line 14-16: This paragraph is absolutely obscure... I don’t understand at all what you are dealing with and description of the equation terms is hard to follow. Be clear, concise, avoid repetition and be simple, that will help. I can’t go further here... Explain clearly how can D be negative and give a clear definition for D ??? What is LIO3Tn? What is MCDn? What is D by the end?

We are very sorry that this “D” parameter confused you and hamper your reading of the manuscript. “D” definition is now clarified (page 7 equations 7 and 8). “r” is the relative difference

between two observations, using the mean value of these 2 observations to not considere anyone as the reference one. "D" is the mean over the entire dataset of the absolute values of "r". We use the absolute values of "r" because positive and negative values can balance each other resulting in an erroneous "D" (which can not be negative indeed - X label of right panel plots of Figures 5 and 6 is now "r" instead of "D").

Line 17 p8 add sondes after ECC.

Done.

Line 23-28 p8 : For that reason I think you should use only 'evaluate' and not 'validate'...as mentioned above.

Following the work of Johnson et al. (2002, 2016) intercomparing various KI and buffer solutions, we found that this ENSCI/0.5% full buffer solution tends to overestimate the amount of ozone by 1.7% in the troposphere. Consequently, an adpated correction was applied on the ECC profiles during this period. This is stated page 7 line 28 and page 8 line 1. Having corrected these ECC observations, we consider we can use them to validate the LIO3T measurements.

Line 9 p9 "SO2 loading too strong" imprecise, please provide informations on the amount.

This aerosol enhancement is clearly visible on the 355nm channels of the stratospheric ozone and LI1200 lidars, and on the 532nm channel of the LIO3T (not shown), and back trajectories together with CALIOP observations (on board CALIPSO - not shown) show that the detected plume comes from the Calbuco volcano. Consequently, although we do not have any information on the corresponding aerosol and SO2 amount, we consider as a wise assumption that, in the layer where this volcanic plume lies (i.e. between 17 and 22km), the SO2 and aerosols loading is too strong to allow a correct O3 retrieval. The study of this volcanic plume crossing in the south-western Indian Ocean will be the subject of dedicated articles. These explanations are added page 8 lines 12-17.

Line 11 p9 : "mean D" see above comment and remove LIO3Tlow which is undefined and that I do not understand. Clear definition is mandatory.

D only gives an absolute relative difference between two datasets, without indicating which one is greater than the other. "LIO3T low" means that the LIO3T dataset gives lower values than the ancillary dataset. It is now made more explicit.

Line 15 p9: "Enhanced" by how much and provide a reference.

These sentences warn the reader about specific conditions that occurred during the MORGANE campaign, and introduce an ongoing work about these stratospheric intrusions above Reunion Island involving the Calbuco volcanic plume. Consequently, no reference is available. This paragraph is modified according to this answer.

Line18-19 p9: Not at the right place, move to conclusions and future plans.

Done.

Figure 8 and 9 : I am not able to make any comment at the moment. Please use different line thickness for the mean and standard deviation in the figures. Text of the figure caption might be improved. Use same Yaxis altitude range in both figures.

Figures 5 and 6 are now improved with respect to these comments.

Line 21-22 p9 : Replace 3PM by 15:00:00 LT, 7PM by 19:00:00 and 1AM by 01:00:00 LT

Done.

Line 25 p9 : replace “goes”

Done.

Line 29-30 p9: rephrase this sentence, unclear.

This sentence is suppressed because the ENSCI/0.5% full buffer solution effect is now corrected.

Line 2 p10 : This FTIR spectrometer should be added to the list of instruments operating at Maïdo Observatory and provided in introduction (line 26-27).

We talk in the introduction only about the “lidar systems that are permanently deployed and routinely operated at the Maïdo Observatory”. As of this writing, 30 instruments are installed in the Maïdo Observatory, and this paper does not aim to list all of them. However, Figure 1 is changed and the FTIR appears on it, together with its location.

Line 19-20 p10 : improve text...both instrument are operating at the same place so their measurements are colocated...What has to be pointed out is the time window you consider for the comparison.

This sentence is made clearer.

Add “Thus, for the LIO3T comparison with FTIR, 114 LIO3T profiles are available”.

114 FTIR-LIO3T pairs are available, because a single LIO3T profile can be linked to several FTIR measurements (within the time window).

Line 21 p10 : just mention the selected LIO3T profiles are regridded consistently to the FTIR.

Done.

Line 22 p10 How many FTIR data are averaged within 24h.

It depends on the measurement conditions (the FTIR only operates in clear daily skies).

Line 23-31 p10: Very very hard to follow...

Sorry about that !

Line 3 p11: replace “time series” by “available over the 01/2013-01/2015 period.”

Done.

Figure 11 : The caption is imprecise and bottom plot Y-axis text is not consistent with equation 6. Is it D???

Y label is now “r”.

Moreover, I found 12 symbols on this bottom plot ???

That is right. Number is changed page 10 line 4.

Figure 12 : I wonder if figure 10 and 12 should be gathered...

Good idea, Figure 10 and 12 are now gathered into Figure 7.

Provide minor ticks for the month on the Xaxis plots

Done.

Line 18 p11 : suppress “ hereabove for the comparison with the ground-based FTIR observations” and replace by “in section 4.2.1”.

Done.

Figure 13: refer to figure 11 comment

Done.

Line 27 p11 : I don't clearly see a seasonal cycle, I see an O3 increase particularly in 2013 and 2016 suggesting an impact of biomass burning...

This sentence is corrected (page 10 line 32).

Section 5 : Title is data set and times series... You are dealing here with data from Intensive period of observations during campaigns... I think it makes the difference with material in previous sections, if I well understood. Please provide a more explicit title. This section is lengthy.

In Section 4, we were dealing with comparison with ancillary data coming from both intensive (Maïdo ECC) and routine (Gillot ECC, FTIR and IASI) periods of observations. In Section 5, we present the full datasets and the resulting climatologies. Section 5 title is changed to "Dataset and climatologies". Moreover, this section is now shortened.

Line 30 p11 – line 3 p12 : You provide LIO3T results in this section...Thus other lidar and details not used further are out of the scope of your study. Thus suppress. This text is very long and the Figure 14 do not provide more informations with respect to the text and is difficult to read. Shorten and improve text.

Text is shorten and Figure 14 is removed because Figure 10 now shows the monthly total number of LIO3T profiles.

Figure 15 is not much informative and text seems to repeat what is given in Line19-21 p7.

Figure 15 is suppressed.

Figure 4 : Please specify in the caption of bottom panel what the LIO3T climatology includes (data routinely performed and from intensive period of observations ???).

It is now specified in the caption that the plot includes data routinely performed and from intensive period of observations

Figure 16 : please provide these informations (4 numbers) on Figure 17 and suppress Figure 16.

Figure 16 is suppressed and information are given in Figure 12 caption.

Line 16-20 p12 : bring in the light what are the benefits from your new lidar...For sure a better description from the upper-troposphere/lower-stratosphere than when located at UR.

Exactly. It is now stated in the text (page 12 lines 18-20).

Line 21-24 p12 : valuable comments and for such reasons I encourage authors to carefully and

rigorously revised the manuscript. Take care to the ECC caveats already mentioned.

OK.

Figure 17 : I recommend to add informations on the seasonal sampling frequency with respect to altitude and this should be done here with an additional panel.

Done on Figure 12 (right panel).

Section 6 : bring more in the light the benefits provided from LIO3T...if monthly climatology from ECC is equivalent and to LIO3TUR and LIO3T (i.e. range of values and seasonal patterns). Could you reinforce you study here... Your goal was to describe the whole tropospheric column with LIO3T... What is your conclusion?

The move of this lidar from the Université de la Réunion campus site up to the Maïdo observatory allows it to document the UT/LS region and to follow stratospheric and tropospheric intrusions with relevant vertical and time resolutions together with a reasonable uncertainty (1.5km, 20min and 14%, respectively, at 18km). This tropospheric ozone data set covering the tropical free troposphere and UT/LS of a sparsely documented region (South Western Indian Ocean) constitutes an extremely valuable resource for the validation of satellite tropospheric ozone retrievals, analysis of the ozone variability and sources, dynamics analysis of case studies, and for long term atmospheric monitoring. This is now stated page 12 lines 18-23.

Line 15-20 p12 : specify altitude range here.

Done.

Line 29-32 p12 : suggestion : A DIAL tropospheric ozone lidar was operating on the Université de la Réunion campus site from 1998 to 2010, providing 427 ozone profiles.

OK.

Note that this information on 427 profiles was not mentioned before. Same remark for LIO3T profiles.

It was mentioned page 4 line 11 for the LIO3TUR and page 12 line 4 for LIO3T.

Replace “familly” by network.

Done.

Line 9 p13 : “we found a 7.7% D between”...revised with the D definition.

Done.

Ozone profiles by DIAL at Maïdo Observatory (Reunion Island) Part 1. Tropospheric ozone lidar: system description, ~~performances evaluation~~ instrumental performance, and result comparison with ~~ancillary~~ ozone external data set

Valentin Duflot[1,2], Jean-Luc Baray[3], Guillaume Payen[2], Nicolas Marquestaut[2], Francoise Posny[1], Jean-Marc Metzger[2], Bavo Langerock[4], Corinne Vigouroux[4], Juliette Hadji-Lazaro[5], Thierry Portafaix[1], Martine De Mazière[4], Pierre-Francois Coheur[6], Cathy Clerbaux[5,6], and Jean-Pierre Cammas[1,2]

[1]Laboratoire de l'Atmosphère et des Cyclones (LACy), UMR8105, Saint-Denis de La Réunion, France
[2]Observatoire des Sciences de l'Univers de La Réunion (OSUR), UMS3365, Saint-Denis de la Réunion, France
[3]Laboratoire de Météorologie Physique (LaMP), UMR6016, Observatoire de Physique du Globe de Clermont-Ferrand, CNRS - Université Blaise Pascal, Clermont-Ferrand, France
[4]Royal Belgian Institute for Space Aeronomy (BIRA-IASB), 3, Av. Circulaire, 1180, Brussels, Belgium
[5]LATMOS/IPSL, UPMC Univ. Paris 06 Sorbonne Universités, UVSQ, CNRS, Paris, France
[6]Spectroscopie de l'Atmosphère, Service de Chimie Quantique et Photophysique, Université Libre de Bruxelles (ULB), Brussels, Belgium

Correspondence to: Valentin Duflot (valentin.duflot@univ-reunion.fr)

Abstract. Recognizing the importance of ozone (O_3) in the troposphere and lower stratosphere in the tropics, a DIAL ~~tropospheric ozone~~ (Differential Absorption Lidar) tropospheric O_3 lidar system (LIO3T$_{UR}$) was developped and installed at the Université de la Réunion campus site (close to the sea) in Reunion Island (southern tropics) in 1998. From 1998 to 2010, it acquired 427 ~~ozone~~ O_3 profiles from the low to the upper troposphere and has been central to several studies. In 2012, the system was moved up to the new Maïdo Observatory facility (2160m above mean sea level - amsl) where it started operation in February 2013. The current system (LIO3T) configuration generates a 266nm beam obtained with the fourth harmonic of a Nd:YAG laser sent into a Raman cell filled up with deuterium (using helium as buffer gas) generating the 289 and 316nm beams enabling the use of the DIAL method for ~~ozone~~ O_3 profile measurements. Optimal range for the actual system is 6-19km amsl, depending on the instrumental and atmospheric conditions; for a 1-hour integration time, vertical resolution varies from 0.7km at 6km amsl to 1.3km at 19km amsl, and mean uncertainty within the 6-19km range is between 6 and 13%. Comparisons with 8 electrochemical concentration cell (ECC) sondes simultaneously launched from the Maïdo Observatory show a good agreement between datasets with a ~~7.7~~6.8% mean absolute ~~value of the relative differences with respect to the mean~~ relative difference (D) between 6 and 17km amsl (LIO3T ~~low~~lower than ECC); comparisons with 37 ECC sondes launched from the nearby Gillot site during day time in a $\pm$ 24-hour window around lidar shooting result in a ~~10.3~~9.4% D between 6 and 19km amsl (LIO3T ~~low~~lower than ECC); comparisons with 11 ground-based Network for Detection of Atmosphere Composition Change (NDACC) Fourier Transform Infrared (FTIR) spectrometer measurements acquired during day time in a $\pm$ 24-hour window around lidar shooting show a good agreement between datasets with a D of 11.8% for the 8.5-16km partial column

(LIO3T ~~high~~higher than FTIR); and comparisons with 39 simultaneous Infrared Atmospheric Sounding Interferometer (IASI) observations over Reunion Island show a good agreement between datasets with a D of 11.3% for the 6-16km partial column (LIO3T ~~high~~higher than IASI). ECC, LIO3T$_{UR}$ and LIO3T O_3 monthly climatologies all exhibit the same range of values and patterns. In particular, the southern hemisphere biomass burning seasonal enhancement, the ozonopause altitude decrease in late austral winter-spring, as well as the signature of deep convection bringing boundary ~~layer-ozone~~ layer-O_3 poor air masses up to the mid-upper troposphere in late austral summer, are clearly visible on all datasets.

1 Introduction

~~Ozone is a major greenhouse gas in the upper troposphere and lower stratosphere~~

Because of its interaction with solar and terrestrial radiation, ozone (O_3) is an important contributor to Earth's radiative balance, and any changes in its atmospheric distribution contribute to the radiative forcing of climate change (Lacis et al., 1990)~~,~~. O_3 is also an important pollutant, and impacts the oxidative capacity of the atmosphere (Martin et al., 2003). In the troposphere, the ~~ozone~~ O_3 budget is influenced by transport from the stratosphere, by in situ photochemical production associated with ~~ozone~~ O_3 precursors emitted by anthropogenic activity, biomass burning, lightning and by surface deposition (Stevenson et al., 2006).

Reunion Island is a tropical island located in the south-western part of the Indian Ocean at 20.8°S and 55.5°E. It is seasonally impacted by biomass burning plumes transported from Southern Africa, South America and South-East Asia which can significantly affect the free tropospheric concentrations of ~~ozone~~ O_3 and other pollutants like CO (Edwards et al., 2006 ; Duflot et al., 2010). Moreover, it is affected by stratospheric intrusions associated with the dynamical influence of the subtropical jet stream (Baray et al., 1998; Clain et al., 2010) and the tropical cyclone deep convection (Leclair de Bellevue et al., 2006).

The barrier effect and dynamical exchanges between the tropical reservoir and midlatitudes, and vertically between the troposphere and the stratosphere~~are~~, affect the O_3 balance and distribution in both the troposphere and stratosphere, and are then of great interest to document climate change. Tropospheric ~~ozone measurements are then~~ O_3 measurements are performed routinely in Reunion Island by ~~ozone~~ O_3 sondes at the Gillot site (~~20.893S, 55.529E, 9m above mean sea level (amsl) ;~~ cf. Figure 1 and Table 1) since 1992 (in the framework of the Network for the Detection of Atmospheric Composition Change - NDACC since 1996 and of Southern Hemisphere ADditionnal OZone sondes - SHADOZ network since 1998), and by lidar at the Université de la Réunion campus site (~~20.902S, 55.485E, 80m amsl~~cf. Figure 1 and Table 1) since 1998 (Baray et al., 1999, 2006).

To improve the ~~operation of~~ ability of the ground-based remote sensing instruments ~~, a 2160m-high~~ to probe the upper-troposphere/lower-(UT/LS) region, a high atmospheric facility was built in 2012 at the summit of the Maïdo mount (~~21.079S, 55.383E, 2160m amsl -~~ cf. Figure 1 and Table 1), and most of the instruments previously installed close to the coast at the Université de la Réunion campus site were moved up to this new facility along the year 2012 (Baray et al., 2013). Being inside the boundary layer during the day and most of the time inside the free troposphere during the night (except during the warm and rainy season), the Maïdo Observatory is dedicated to the investigation of the boundary layer composition and processes (especially

in the framework of the Global Atmospheric Watch network - GAW), as well as to the study of the low-middle atmosphere (especially in the framework of the NDACC). Four lidar systems are permanently deployed and routinely operated at the Maïdo Observatory:

- a Doppler wind lidar dedicated to the study of the middle atmosphere dynamics (Khaykin et al., 2015),
- the LIO3S, a lidar dedicated to stratospheric ~~ozone~~ O_3 measurements (Portafaix et al., 2003; Portafaix et al., 2015),
- the LI1200, a lidar dedicated to tropospheric water vapor (Hoareau et al., 2012; Dionisi et al., 2015; Vérèmes et al., 2015, 2017) and stratospheric-mesospheric temperature measurements (Morel et al., 2002; Keckhut et al., 2004, 2015; Sivakumar et al., 2011a),
- and the LIO3T lidar (Baray et al., 1999~~; Keckhut et al., 2004; Baray et al.,~~ , 2006; Clain et al., 2009, 2010; Vérèmes et al., 2016) dedicated to the observation of tropospheric ~~ozone~~ O_3 (as well as aerosols from the free troposphere up to the lower stratosphere).

It is noteworthy that the LIO3T system was very recently affiliated in the NDACC for ~~ozone~~ O_3 measurements ; this paper aims to provide a technical reference socle for further use of the ~~ozone~~ O_3 data provided by the LIO3T system: we first present the data processing, we then give a brief historical review of the tropospheric ~~ozone lidar system and measurements performed~~ O_3 lidar system when installed at the Université de la Réunion campus site (1998-2010) ~~, we then describe~~ together with a description of the current LIO3T system installed at the Maïdo Observatory. We show comparisons between the LIO3T ~~ozone~~ O_3 measurements and ancillary data~~, and we~~ . We finally present an overview of the ~~2013-2015 Maïdo Observatory ozone measurements~~ lidar tropospheric O_3 profiles database.

In the following, the system will be referred as "LIO3T$_{UR}$" when it was installed at the Université de la Réunion~~(for LIdar O_3 Tropospheric Université de la Réunion)~~, and the current system (installed at the Maïdo Observatory) will be referred as "LIO3T".

2 ~~Brief historical review of the lidar system at the Université de la Réunion campus site (1998-2010)~~Data processing

~~This section aims to provide a review of the LIO3T$_{UR}$ system and resulting dataset. It gives an overview of the historical context preceding the operation of the tropospheric ozone lidar at the Maïdo Observatory. It also presents the main characteristics of the LIO3T$_{UR}$ system, its performances and database, and shows a compilation of the resulting observations over the 13 years of operation from 1998 to 2010.~~

2.1 ~~Instrumental set up and technical choices~~

~~A Rayleigh-Mie lidar was first installed at the Université de la Réunion campus site in 1993 to monitor stratospheric and mesospheric aerosols in the southern tropics. From 1993 to 1998, the lidar system evolved both in terms of emission and reception (Nd:YAG laser replacement, mosaic telescopes addition, polarization channels installation, infrared channel reception set up) to improve aerosols detection and characterization, and to allow stratospheric-mesospheric temperature measurement.~~

In 1998, a tropospheric ozone extension was installed to the existing system (Baray et al., 1999). The goal was to perform ozone measurements over the entire tropospheric column, including the upper troposphere. To achieve this, the 289 and 316nm wavelengths pair was chosen because it affords a good trade-off among the needs for sensitivity in both free troposphere and tropopause region and sufficient laser energy at the implied Raman Stokes lines. The 266nm beam obtained with the fourth harmonic of the Nd:YAG laser was therefore sent into a Raman cell filled up with deuterium generating the 289 (1st Stokes) and 316nm (2nd Stokes) beams enabling the use of the DIAL method for ozone profilemeasurements. After collection through telescopes and optical fibers, the 289 and 316nm signals were spectrally separated with a spectrometer that includes a Czerny-Turner holographic grating and sent toward Hamamatsu R1527P PMTs. An analog channel was used for the lower layers and a photoncounting channel for the mid- and upper troposphere. Baray et al. (1999) give a complete description of the 1998 system and provide justifications of the technical choices that were made at this time. Note that the first "home made" acquisition chain was changed for a LICEL one in 2007, but this change did not cause significant differences in the profiles acquired.

The description of the well-known DIAL retrieval scheme of the ozone profile from the backscattered ON (absorbed by ozone, here: 289nm) and OFF (less absorbed by ozone, here: 316nm) signals can be found in, e. g., Pelon and Mégie (1982) and Mégie et al. (1985). Molina and Molina (1986) ozone cross sections were used for ozone profile retrieval.

2.1 Performances, dataset and ozone climatology

The LIO3T$_{UR}$ optimal range was 3.5-17km amsl. Figure 2 gives the mean uncertainty and resolution over the 13 years of operation. The mean uncertainty varies from 6% at 3km amsl to almost 60% at 17km amsl. Vertical resolution goes from 0.1km at 3km amsl to 1.8km at 17km amsl. The temporal resolution (or integration time) was chosen depending on the atmospheric conditions and varied roughly between 40 minutes and 3 hours. Figure 3 shows the number of acquired profiles per year from 1998 to 2010. 427 tropospheric ozone profiles were acquired over the 13-year operation period. Measurements were stopped in 2010 to prepare the move up to the Maïdo Observatory.

Figure 4 (top right panel) shows the resulting monthly tropospheric ozone climatology. For comparison, the monthly tropospheric ozone climatology derived from the electrochemical concentration cell (ECC) sondes measurements performed at the Gillot site (Figure 1) between 2005 and 2015 is shown (top left panel). Note that for comparison convenience, whereas Maïdo Observatory tropospheric ozone system, retrieval, performances and database descriptions are the subject of the following sections, the tropospheric ozone monthly climatology resulting from the lidar observations at the Maïdo Observatory is also plotted on Figure 4 (bottom panel) but will be discussed only in Section 5. We focus here on the description and comparison of the ECC and LIO3T$_{UR}$ climatologies (Figure 4, top panels) in order to estimate the consistency between datasets and to highlight the main climatological patterns.

The following seasonal features can be observed on both ECC and LIO3T$_{UR}$ climatologies:

- a clear increase of ozone abundance over the whole tropospheric column - especially between 2 and 10 km amsl - starting in June and ending in December with a maximum in October of $\approx 10x10^{11}$ molec/cm^3 on average between 4 and 10 km amsl; this increase is due to the influence of air masses coming from South America, Southern Africa and South-East Asia (Edwards

et al., 2006; Duflot et al., 2010) where the biomass burning season occurs every year during this period; ozone abundance then presents a slow decay over the entire tropospheric column from January to May;

- the ozonopause altitude decrease from ≈ 17 km in December-July down to ≈ 15 km amsl in August-November (Sivakumar et al., 2011b), which is likely a combination of the spring and summer maximum of occurrence of stratosphere-to-troposphere exchanges (STE) above Reunion Island (Clain program used to calculate the O_3 profile, uncertainties and resolution is adapted from the stratospheric O_3 program "DIAL", which has been described and inter-compared by Godin et al. , 2010) and of the winter time thermal effect on the troposphere thickness.

3 The current tropospheric ozone system at the Maïdo Observatory (2013-present)

Late 2012, the Maïdo Observatory new facility was complete and many instruments were moved from the Université de la Réunion campus site and installed in the Observatory. Since temperature measurements are now performed with another lidar system - also dedicated to water vapor measurement (Dionisi et al., 2015; Vérèmes et al., 2015) - the previous LIO3T$_{UR}$ was modified into a system dedicated to the measurement of tropospheric ozone (and aerosols): the "LIO3T".

2.1 Description of the current system

We focus here only on the DIAL ozone part of the LIO3T system. Figure 5 sketches the experimental schematic of the ozone DIAL part of the LIO3T and Table 1 gives its main technical characteristics. The LIO3T system mainly relies on the LIO3T$_{UR}$ design (Baray et al., (1999) . We use the same approach to generate a 266nm beam going through a deuterium filled Raman cell (using helium as buffer gas) shifting the incoming frequency to 289 and 316nm signals. Operating at a repetition rate of 30 Hz, the 266nm UV pulse energy is currently around 40 mJ per pulse. Backscattered photons are collected by a 4x500mm-telescope mosaic focusing on 1.5mm diameter optical fibers. The optical system allows to obtain an image quality (pulse response of a star image located at the infinite) associated to the atmospheric turbulence of 0.8 mrad. Concerning the part associated to the quality of the receiving telescopes, 90% of the energy is included in 0.6 mrad. After a system of three lenses used to reduce the divergence of the beam by a factor 3, and to adapt the numerical aperture of fibers to that of the grating, the spectral separation of the 289 and 316 nm beams is obtained by a high performance Czerny-Turner holographic grating (3600 lines/mm). Then each beam is redirected towards photomultiplier tubes (PMT) by concave mirrors. Hamamatsu R9980-110 and R7400P-03 photomultipliers tubes are used, for 289 and 316 nm channels, respectively. A Licel time-correlated photon counting unit is used to discriminate both channels energy-shifted photons, triggered by the optical laser signal at 30 Hz with a 150 m resolution. is currently used for the stratospheric DIAL O_3 retrievals at Reunion (NDACC affiliated).

For information, the detection and characterization of the tropospheric aerosols by the LIO3T system is currently performed using the emitted 532nm "residual" beam, a 200mm telescope for reception of the elastic signal, and a polarization detection system. This aerosols detection wing of the LIO3T system will be the subject of dedicated studies.

2.1 Lidar equation

2.2 ~~Data processing~~

2.1.1 ~~Lidar equation~~

The lidar DIAL (Differential Absorption Lidar) technique (Hinkley, 1976) relies on the difference between two backscattered lidar signals at two different wavelengths, one ~~being relatively strongly~~ where O_3 is strongly absorbed (ON, here: 289nm) ~~absorbed by the target species, the other one being relatively weakly absorbed~~ and the other one where O_3 absorption is weaker (OFF, here: 316nm). The ~~ozone~~ O_3 number density $n_{O3}(z)$ at altitude z (in molec/cm^3) is retrieved from the Rayleigh lidar signals according to the following equation:

$$n_{O3}(z) = \frac{-1}{2\Delta\sigma_{O3}(z)} \frac{d}{dz}\left[ln\left(\frac{P(\lambda_{ON},z) - B(\lambda_{ON},z)}{P(\lambda_{OFF},z) - B(\lambda_{OFF},z)}\right)\right] + \delta n_{O3}(z) \quad (1)$$

where $\Delta\sigma_{O3}(z) = \sigma_{O3}(\lambda_{ON},z) - \sigma_{O3}(\lambda_{OFF},z)$ is the differential ~~ozone~~ O_3 absorption cross-section~~at altitude z~~, $P(\lambda_i,z)$ is the number of detected photons~~at the wavelength λ_i and at the altitude z~~, $B(\lambda_i,z)$ is the background noise and detector noise~~at the wavelength λ_i and at the altitude z~~, and $\delta n_{O3}(z)$ is a correction term corresponding to the absorption by other constituents of the atmosphere, expressed as follows:

$$\delta n_{O3}(z) = \frac{1}{\Delta\sigma_{O3}(z)}\left[\frac{1}{2}\frac{d}{dz}\left[ln\left(\frac{\beta(\lambda_{ON},z)}{\beta(\lambda_{OFF},z)}\right)\right] - \Delta\sigma_{atm}(z)n_{atm} - \sum_{ig}\Delta\sigma_{ig}(z)n_{ig}(z)\right] \quad (2)$$

where $\beta(\lambda_i,z)$ is the coefficient of extinction of the molecules and particles~~at the wavelength λ_i and at the altitude z~~, $\Delta\sigma_{atm}(z)$ and n_{atm} the differential cross-section and the density of the atmosphere~~at the altitude z~~, respectively, and $\Delta\sigma_{ig}(z)$ and $n_{ig}(z)$ the differential cross-section and the number density of interfering gas ig~~at the altitude z~~, respectively. ~~The~~ According to Leblanc et al. (2016b), the interfering gases to consider in practice are NO_2, SO_2, and O_2. NO_2 and SO_2 are negligible in most cases of tropospheric O_3 retrieval, except in heavy volcanic aerosols loading conditions. The absorption by O_2 should be considered if any of the detection wavelength is shorter than 294nm (which is the case here as we use the 289nm wavelength). However, in our case, we do not take into account in our retrieval any interfering gases for the time being. It is part of our future plans to include them in the "DIAL" code. The background light, the saturation of the detector and the noise from detectors must be added to this equation (2).

2.1.1 ~~Desaturation, filtering and vertical resolution~~

2.2 Saturation, correction and vertical resolution

~~Saturation can occur~~ The saturation is defined as a difference between the number of photons received by the detector and the number of photons acquired. It is a non-linear phenomenon, depending on the dead time of the detector. When this saturation

is low, it is possible to use a formula to calculate the number of photons received. Several definitions of the desaturation exist (e.g. Donovan et al., 1993), we apply the formula described in Pelon (1985, Annex 2):

$$N_c = 1 + \left[\left(1 - \frac{\tau}{\delta t}\right) N_r - 1\right] e^{-\frac{\tau}{\delta t} N_r} \quad (3)$$

with N_c the number of photons counted, N_r the number of photons received, τ the dead time of the detector and δt the integration time. In the LIO3T case, due to the detector sensitivity and the geometry of the instrument, we found that saturation occurs only below 7km~~amsl~~. To correct it, we apply the scheme described in Pelon (1985, Annex 2). To calculate equations (1) and (2), we apply a derivative filter, which can be expressed as:

$$S_f(k) = \sum_{n=-N}^{N} c_n S(k+n) \quad (4)$$

where $S_f(k)$ is the filtered signal, $S(k)$ is the signal to be filtered and c_n the filter coefficients. These coefficients define the type of filter ~~:~~ such as low-pass ~~, derivatives, etc~~and derivatives. Increasing the number of points of the filter reduces the noise in the signal but degrades the vertical resolution. The calculation of the vertical resolution from the filter parameters is ~~described~~ extensively detailed in Leblanc et al. (2016a). In our case, we use the frequency approach: we calculate the transfer function of the filter and we ~~decide~~ found that the frequency for which the gain is lower than 0.5 is the cut-off frequency (not shown). We obtain the vertical resolution by dividing the initial resolution by the cut-off frequency. We use the Savitzky-Golay filter of order 2, also called least-squares smoothing filter (Savitzky and Golay, 1964). The ~~resolution rises~~ vertical resolution decreases with the altitude according to a polynomial function (cf. Section ~~3.3 and Figure 6~~3.2 and Figure 3).

2.2.1 ~~Uncertainty~~

2.3 Uncertainty

Uncertainties calculation for DIAL ~~ozone~~ O_3 retrievals are described in Leblanc et al. (2016b). The most significant sources of uncertainties are found to be the detection noise, the ~~ozone~~ O_3 cross section uncertainties and the background noise.

The detection noise can be estimated as a Poisson noise because we use our acquisition card in photo counting mode. The associated error is:

$$\sigma_s(z) = \sqrt{s(z)} \quad (5)$$

where $\sigma_s(z)$ is the error of signal s at the altitude z, and $s(z)$ the signal at the altitude z. ~~The used ozone cross-sections are defined by~~ Molina and Molina (1986) and Bass and Paur (1984) O_3 cross sections were used for O_3 profile retrieval for LIO3T$_{UR}$ and LIO3T, respectively, both with an uncertainty equal to 5%.

The background noise includes the background light, which is altitude-independent, and the detector noise - dark noise and induced signals -, which are altitude-dependent. We use then a linear or polynomial regression to remove the background noise.

To take into account the propagation of these errors in the lidar equation, we use the following equation of propagation:

$$\begin{cases} y = f(x_1, x_2, ..., x_N) \\ \sigma_y = \sum_{n=1}^{N} \left(\frac{\partial y}{\partial x_n} \right)^2 u_n^2 \end{cases} \quad (6)$$

where y is the signal depending on variable x_i, σ_y the error of the signal y, $\frac{\partial y}{\partial x_n}$ the derivative of y with respect to the variable x_i, and u_i the uncertainty of x_i. In this equation, we suppose that all uncertainties are independent.

~~The program used to calculate the ozone profile, uncertainties and resolution is adapted from the stratospheric ozone program "DIAL", which has been described and inter-compared by Godin~~

3 Instrumental description and performances

3.1 Historical context and main instrumental features

A Rayleigh-Mie lidar was first installed at the Université de la Réunion campus site in 1993 to monitor stratospheric and mesospheric aerosols in the southern tropics. From 1993 to 1998, the lidar system evolved both in terms of emission and reception (Nd:YAG laser replacement, mosaic telescopes addition, polarization channels installation, infrared channel reception set up) to improve aerosols detection and characterization, and to allow stratospheric-mesospheric temperature measurement.

In 1998, an extension was installed to the existing system to perform O_3 measurements in the free troposphere, including the upper troposphere. Baray et al. (1999) ~~and is currently used for the stratospheric DIAL ozone retrievals at Reunion (NDACC affiliated). In this new tropospheric ozone version, cross-sections are adapted to the used wavelengths, and the uncertainty on these ozone cross-sections is taken into account~~give a complete description of the LIO3T$_{UR}$ and provide justifications of the technical choices that were made at this time. Note that the first "home made" acquisition chain was changed for a LICEL one in 2007, but this change did not cause significant differences in the profiles acquired.

~~Future plans for the data processing are to: i) use the Brion-Daumont-Malicet (Daumont~~ Late 2012, the Maïdo Observatory new facility was complete and the fixed lidar systems were moved from the Université de la Réunion campus site and installed in the Observatory. Since temperature measurements are now performed with the LI1200 system - also dedicated to water vapor measurement (Dionisi et al., ~~1992; Brion~~ 2015; Vérèmes et al., ~~1993; Malicet et al., 1995) ozone cross sections as recommended by the NDACC lidar working group; ii) calculate the uncertainty on the retrieved ozone profile due to the desaturation scheme (which should increase our uncertainty only below 7 km amsl); iii) use the International Space Science Institute (ISSI) team standardized approach for the propagation of the background and saturation corrections uncertainties (Leblanc~~ 2015, 2017) - the previous LIO3T$_{UR}$ was modified into a system dedicated to the measurement of tropospheric O_3 (and aerosols): the "LIO3T".

Figure 2 sketches the experimental schematic of the O_3 DIAL part of the LIO3T and gives its main technical characteristics. The LIO3T mainly relies on the LIO3T$_{UR}$ design (Baray et al., ~~2016b); iv) implement uncertainties calculation due to the presence of aerosols in the troposphere using an iterative aerosol assessment procedure and simultaneous aerosols lidar measurements at~~ 1999). We use the same approach to generate a 266nm beam going through a deuterium filled Raman cell (using helium as buffer gas) shifting the incoming frequency to 289 and 316nm signals, and the backscattered photons are collected by the same 4x500mm-telescope mosaic focusing on 1.5mm diameter optical fibers. Hamamatsu R9880-110 and R7400P-03 photomultipliers tubes are used, for 289 and 316 nm channels, respectively. Further details on the LIO3T features can be found in Baray et al. (2013).

For information, the detection and characterization of the tropospheric aerosols by the LIO3T is currently performed using the emitted 532nm "residual" beam, a 200mm telescope for reception of the elastic signal, and a polarization detection system. This aerosols detection wing of the LIO3T will be the subject of dedicated studies.

3.2 Performances

The LIO3T$_{UR}$ was only operated at night to increase the signal-to-noise ratio. Due to the overlap factor and detection limit, the LIO3T$_{UR}$ optimal range was 3.5-17km above mean sea level (amsl). Note that in the following all altitudes will be given amsl. Figures 3 and 4 give the mean vertical resolution and uncertainty profiles for LIO3T$_{UR}$ over the 13 years of operation. The temporal resolution (or integration time) depended on the atmospheric conditions (i.e. the cloud free sky duration) and varied roughly between 40 minutes and 3 hours. Vertical resolution varies from 0.1km at 3km to 1.8km at 17km. The mean uncertainty varies from $\approx$ 6% ($\approx$ 3.8 x 10e10 molec/cm^3) at 3km to $\approx$ 15% ($\approx$ 7 x 10e10 molec/cm^3) at 16km, and increases up to 60% ($\approx$ 3.5 x 10e11 molec/cm^3) at 17km (not shown) where the detection noise dominates.

The altitude of the Maïdo ~~Mount~~ Observatory being 2160m~~amsl~~, the transfer of the tropospheric ~~ozone~~ O_3 DIAL system from the University (80m~~amsl~~) to this location increases the upper limit of the profile probed, but also increases the lower limit: the optimal range is now 6-19km~~(compared to 3.5-17 km range for the LIO3T$_{UR}$)~~. The free troposphere, the tropical tropopause layer (TTL) and lower stratosphere are thus covered by the current system. It is worth mentioning, however, that depending on experimental conditions (lidar alignment, stability of emitted power ~~, laser and Raman cell,~~ at the transmitted wavelength, atmospheric conditions, etc.), the validity domain can vary from one day to another.

~~The~~ Similarly to the LIO3T~~system~~ $_{UR}$, the LIO3T is only operated at night ~~,~~ to increase the signal-to-noise ratio, and twice a week in routine conditions (i.e. out of campaigns). We use three main integration times: 20 minutes for night time series, 1 hour for comparison with collocated ECC soundings (1 hour is roughly the time for the balloon to travel the troposphere), and $\approx$ 3 hours (between $\approx$ 2 and $\approx$ 4 hours, depending on the clear sky time duration) for "full night" profiles. Figure ~~6 presents examples of resulting profiles and corresponding resolutions for these three integration timesfor the same night (9th July 2013). Ozone vertical distributions and resolutions differ notably when considering the different integration times, the first one - obviously - because of the tropospheric ozone variability, the latter because of the choice of the filtering coefficients.~~ 3 shows the vertical resolution resulting from each of these integration times. For the 20-minutes integration time, the resulting

resolutions are 0.9 and 1.6 km at 6 and 19 km~~amsl~~, respectively; for the 1-hour integration time, they are 0.7 and 1.3 km at 6 and 19 km~~amsl~~, respectively; and for the 3-hour integration time, 0.4 and 1.2 km.

Figure ~~7~~ 4 shows the mean uncertainties for the three main integration times ~~. Unsurprisingly, we find greatest mean uncertainties for the shortest integration time. For the 1- and >1-hour~~ in % (left panel) and molec/cm^3 (right panel). For the three integration times, mean uncertainty ~~goes from 6% at~~ varies between ≈ 7% (≈ 6 ~~and~~ x 10e10 molec/cm^3) at 6km and ≈ 5% (≈ 5.5-8 x 10e10 molec/cm^3) at 19km ~~amsl to 13% at 14km amsl, and for the~~ with a peak at ≈ 10% (≈ 5 x 10e10 molec/cm^3), ≈ 12% (≈ 6 x 10e10 molec/cm^3) and ≈ 15% (≈ 7.5 x 10e10 molec/cm^3) at 16km for the >1 hour, 1 hour and 20 ~~min~~ minutes integration time, ~~the mean uncertainty goes from 7% at 6km amsl to 16% at 16.5km amsl~~respectively. These figures are in agreement with the recently published work of Leblanc et al. (2016b) showing uncertainty profiles for DIAL tropospheric ~~ozone~~ O_3 measurements between 7 and 11%. One can notice that the LIO3T$_{UR}$ uncertainty is higher than the LIO3T one above 16km, while the LIO3T uncertainty decreases (in %) between 16 and 19km. This is due to the fact that the LIO3T$_{UR}$ reaches its detection limit between ≈ 16km and ≈ 17km, while for the LIO3T the detection noise increase is balanced by the O_3 abundance increase when entering the stratosphere.

4 ~~Comparisons~~

4 Comparisons of LIO3T measurements with ancillary data

The goal of this section is to validate the LIO3T ~~ozone~~ O_3 measurements by comparing them to ancillary data. Four types of correlative data are used here: collocated ECC soundings (i.e. launched from the Maïdo Observatory during a lidar shooting), routine NDACC/SHADOZ ECC soundings performed during daytime at the Gillot site (cf. Figure 1 and Table 1), and Fourier Transform InfraRed spectrometer (FTIR) tropospheric partial columns measurements from both daytime ground-based and nighttime ~~space-borne instruments~~Infrared Atmospheric Sounding Interferometer (IASI) data.

In the following, we compare N LIO3T ~~ozone~~ O_3 measurements M_{LIO3T} with N correlative data M_{CD} by calculating the mean absolute ~~value of the relative differences with respect to the mean~~ relative difference between datasets D (in %) defined as:

$$D = \frac{1}{N}\sum_{n=1}^{N}|r_n| \tag{7}$$

with r_n the relative difference (in %) between two observations M_{LIO3T_n} and M_{CD_n} defined as:

$$Dr_n = \frac{200}{N}\sum_{n=1}^{N}\frac{|M_{LIO3T_n} - M_{CD_n}|}{M_{LIO3T_n} + M_{CD_n}} 100 * \frac{M_{LIO3T_n} - M_{CD_n}}{\frac{M_{LIO3T_n}+M_{CD_n}}{2}} \tag{8}$$

4.1 Comparison with ECC

ECC sondes measure the oxidation of a potassium iodine (KI) solution by O_3 (Komhyr et al., 1995). Their accuracy is 5-10% throughout the troposphere and TTL (Smit et al., 2007) and they are commonly used for the validation of ground-based and space-borne ozone O_3 observations. Here below, we compare LIO3T ozone O_3 profiles with both collocated Maïdo ECC soundings and Gillot SHADOZ/NDACC routine daytime ECC soundings. All these ECC profiles are generated following the "Guidelines for homogenization of ozonesonde data" (Smit et al., 2012). The Gillot SHADOZ/NDACC reprocessed ECC dataset was recently presented by Posny et al. (2016)and , Smit et al. (2016) . One caveat should be kept in mind: these ECC soundings were performed and Witte et al. (2017) and is used in this article. Moreover, similar reprocessing was applied on the ECC soundings performed at the Maïdo Observatory. From August 2007 to December 2016, ECC soundings were performed at Reunion Island using the ENSCI/0.5% full buffer solution, instead of the standard half buffer. As of this writing, there is no transfer function to convert these ozone profiles - using non-standard ECC This specificity of the Reunion Island ECC soundings is not taken into account in the SHADOZ/solution pairing - to the standards. The only certitude is NDACC reprocessed ECC dataset yet. Following the work of Johnson et al. (2002, 2016) intercomparing various KI and buffer solutions, we found that this ENSCI/0.5% full buffer solution tends to overestimate the amount of ozone by a few percents in the troposphere (Johnson et al. , 2002). As a consequence, these ECC profiles should be considered as preliminary data and the *D* between them and LIO3T profiles stated hereafter is most probably slightly overestimatedO_3 by 1.7% in average in the troposphere. Consequently, an adapted correction was applied on the ECC profiles acquired during this period.

Figure 8

Figure 5 shows the comparison between LIO3T and collocated ECC soundings: two were performed in June 2013, four in May 2015 and two in July 2015. Note that these last six were part of the Maïdo ObservatoRy Gaz and Aerosols Ndacc Experiment (MORGANE) campaign that took place in May-July 2015 (Portafaix et al., 2015; Vérèmes et al., 2015, 2017; Duflot et al., 2016a; Posny et al., 2016). The integration time for the LIO3T profiles used here is 1h and corresponds roughly to the time for the balloon to travel the troposphere. Note that the "discontinuities" in the mean profiles shown on Figure 8 are caused by the varying valid ranges in the LIO3T profiles (cf. Table 2), and note that no profile goes above 17km for these eight comparisons. In particular, the valid range in May and July 2015 (during the MORGANE campaign) is bounded up at 17km by the strong volcanic aerosol loading coming from the Calbuco volcano, which erupted late April 2015 and whose volcanic plume reached the TTL above Reunion Island on the 6th May 2015 before slowly vanishing until near the end of July 2015 (Bègue et al., 2016). In the This aerosol enhancement is clearly visible on the 355nm channels of the stratospheric O_3 and LI1200 lidars, and on the 532nm channel of the LIO3T (not shown), and back trajectories together with CALIOP observations (on board CALIPSO - not shown) show that the detected plume comes from the Calbuco volcano. Consequently, although we do not have any information on the corresponding aerosol and SO_2 amount, we consider as a wise assumption that, in the layer where this volcanic plume lies (i.e. between 17 and 22km), we consider that the SO2 the SO_2 and aerosols loading is too strong to allow a correct O_3 retrieval (Ancellet et al., 1987; MacGee McGee et al., 1993). The study of this volcanic plume crossing in the south-western Indian Ocean will be the subject of dedicated articles.

One can see on Figure ~~8~~ 5 that there is an overall agreement between LIO3T and the ECC considering the lidar uncertainty and ECC accuracy (right ~~). The mean~~ panel). D is ~~7.7% for~~ 6.8% for the whole probed column (LIO3T ~~low~~lower than ECC). This value agrees with the ones recently reported for single or multiple ECC-lidar comparisons (between 6 and 20% reported by Uchino et al., 2014; 20% reported by Sullivan et al., 2015; 8% reported by Gaudel et al., 2015).

Stratosphere-to-troposphere exchanges were observed above Reunion Island in May 2015 during the MORGANE campaign (Duflot et al., 2016a,b). Enhanced aerosol loadings (likely coming from the Calbuco eruptions) were observed with the 532nm backscattered signal of the LIO3T (not shown) in these stratospheric air masses entering the troposphere above Reunion Island, which could have disturbed the ~~ozone~~ O_3 detection and quantification by the LIO3T~~system~~, and consequently lower the agreement between LIO3T and ECC soundings during this period. ~~Future consideration of the LIO3T simultaneous aerosols measurements in the data processing scheme should help to improve the related uncertainties on the retrieved O_3 profiles~~These stratosphere-to-troposphere exchanges involving a volcanic plume above Reunion Island will be the subject of a dedicated study.

Figure ~~9~~ 6 shows the comparison between the SHADOZ/NDACC Gillot routine ECC soundings and LIO3T profiles. As the first ones are performed during daytime (usually around ~~3PM local time~~15:00:00 LT) and the last ones during night time (between ~~7PM and 1AM local times~~19:00:00 and 01:00:00 LT), ECC soundings are taken into consideration when performed one day before or after a LIO3T profile acquisition; we find 37 pairs for comparison over the years 2013-2015. The LIO3T profiles used here are "full night" profiles. Once again, note that the "discontinuities" in the mean profiles shown on Figure ~~9~~ 6 are caused by the varying valid ranges in the LIO3T profiles (and one can see that only one profile ~~goes~~ is above 18km). Despite the fact that the instruments were neither collocated in time nor space (the ECC launch site - Gillot - is ~~≈ 20km~~ 26km away from the Maïdo Observatory (cf. Table 1) and balloons are advected by the wind), one can see that there is an overall good agreement between measurements considering the lidar uncertainty and ECC accuracy, with a mean D equal to ~~10.3~~9.4% over the entire 6-19km column (LIO3T ~~low~~lower than ECC).

~~One should remind that these very satisfactory agreements between ECC and LIO3T profiles should slightly improve in the future when a transfer function to convert these ECC ozone profiles to the standards is set up.~~

4.2 Comparison with ground-based and space-borne FTIRs

In this section we compare the LIO3T ~~O_3~~ profiles with collocated partial column measurements performed by two FTIRs: the Bruker 125HR installed at the Maïdo Observatory since 2013, and ~~the Infrared Atmospheric Sounding Interferometer (IASI)~~ IASI on board the MetOp-A satellite.

4.2.1 Comparison with NDACC ground-based FTIR measurements

A Bruker 125HR FTIR spectrometer started operating at the Maïdo Observatory in March 2013 with a primary dedication to NDACC measurements (Zhou et al., 2016). This NDACC ground-based FTIR observes the absorption of the direct solar radiation with high spectral resolution (0.0035-0.0110 cm^{-1}) and uses the pressure broadening effect of absorption lines to retrieve volume mixing ratio (vmr) low vertical resolution profiles of target gases. The FTIR ~~ozone~~ O_3 measurements show a

good sensitivity from the ground up to about 45 km. Within this vertical range, about 4 vertical layers can be distinguished, i.e. the vertical resolution varies from 8 to 15 km (Vigouroux et al., 2015). In this study, the FTIR retrievals are based on an optimal estimation method (Rodgers, 2000), carried out with the SFIT4 algorithm (https://wiki.ucar.edu/display/sfit4), which is an open source code, jointly developed at the NASA Langley Research Center, the National Center for Atmospheric Research (NCAR), the National Institute of Water and Atmosphere Research (NIWA) and University of Bremen. HBr cell measurements are performed on a daily basis to verify the alignment of the instrument and to obtain the instrument line shape (ILS) using the LINEFIT14.5 program (Hase et al., 1999). The retrieval scheme is described in Vigouroux et al. (2015), and closely follows the recipe of the Jungfraujoch station (except for the ILS which is fixed from LINEFIT results at Maïdo): the retrieval microwindow is 1000-1005 cm^{-1}, the a priori data comes from the WACCMv6 model and pressure and temperature a priori profiles were obtained from National Centers for Environmental Prediction. The a priori water profile is obtained from a dedicated pre-retrieval. Each ~~ozone~~ O_3 profile is retrieved with the signal to noise of the source spectrum. The total uncertainty on the ~~ozone~~ O_3 profile is dominated by the smoothing error (i.e. the poor vertical resolution of the profile), the temperature and the spectroscopic uncertainties. We use the following approach for comparison:

i) FTIR performing observations during daytime, each LIO3T measurement is ~~co-located~~ compared to all FTIR measurements within a 24-hour time window;

ii) for each such a pair (114 pairs in total), the LIO3T profile is regridded ~~(with mass conservation)~~ consistently to the FTIR~~height grid~~;

iii) FTIR measurements are averaged within the 24-hour time window around a single LIO3T measurement for comparison;

iv) at this stage we have a set ~~a~~ of comparable pairs of measurements with various validity domain for LIO3T profiles; however, the method needs constant boundaries for the partial column used for comparison; we then choose the partial column shared by a sufficient number of LIO3T profiles to allow a reasonable comparison; the upper and lower limits of this partial column are called hereafter "valid range for comparison";

v) the regridded LIO3T profile is smoothed with the FTIR averaging kernel matrix and a priori (see, e.g., Rodgers and Connor, 2003; Vigouroux et al., 2008); to allow for the smoothing, the LIO3T measured profiles are extended by the FTIR a priori outside the valid range for comparison. By smoothing the LIO3T profiles, we degrade them to the FTIR low vertical resolution, and we can get rid of the FTIR smoothing uncertainty in the uncertainty associated with the comparison;

vi) finally, a partial column is calculated from this smoothed LIO3T profile in the valid range of comparison.

We find ~~11~~ 12 comparison pairs over the studied period within the 8.5-16km valid range for comparison. In this 8.5-16km partial column, the ground-based NDACC FTIR has 1.1 degree of freedom (Rodgers, 2000) and a mean total uncertainty of 7.5%. Figure ~~10~~ 7 shows the FTIR a priori profile and averaging kernels for this 8.5-16km partial column, both of them being used to smooth the LIO3T measurements to compare with the FTIR ones.

Figures ~~11~~ 8 shows the comparison of the FTIR and LIO3T partial columns ~~time series~~available over the 01/2013-01/2016 period. One can see that there is a good agreement between the datasets considering the uncertainties. We find a D of 11.8% between datasets (LIO3T ~~high~~higher than FTIR). Note that, due to the sparse comparison points, the southern hemisphere biomass burning season is not visible on this plot.

4.2.2 Comparison with IASI measurements

IASI is on board the MetOp-A satellite launched in a Sun-synchronous orbit around the Earth at the end of 2006. A second IASI was launched on board MetOp-B in September 2012 and the launch of the third one (MetOp-C) is planned for late 2018. In this comparison, IASI/MetOp-A data are used. IASI is a FTIR instrument that measures the thermal infrared radiation emitted by the Earth's surface and atmosphere in the 645-2760 cm^{-1} spectral range with a spectral resolution of 0.5 cm^{-1} apodized and a radiometric noise below 0.2K between 645 and 950 cm^{-1} at 280K (Clerbaux et al., 2009).

IASI is an interesting instrument for our intercomparison effort as it provides global Earth coverage twice daily with overpass times at 09:30:00 and 21:~~30MLT (~~30:00 mean local time ~~)~~ and a nadir footprint on the ground of ~~12 km~~12km. IASI has significant sensitivity to tropospheric O_3. As LIO3T usually fires between ~~7PM and 1AM~~ 19:00:00 and 01:00:00 local times, we used here the IASI nighttime overpass measurements. The IASI data used in this study come from the FORLI-O_3 v20151001 scheme (Hurtmans et al., 2012; Boynard et al., 2016).

To compare measurements from both instruments, IASI retrievals are averaged over a 1°x1°box around the Maïdo Observatory location. We then use the same approach as described ~~hereabove for the comparison with the ground-based FTIR observations~~ in Section 4.2.1 (except points i) and iii)). We find 39 comparison pairs over the studied period within the 6-16km valid range for comparison. In this 6-16km partial column, IASI has 1.6 degree of freedom (Rodgers, 2000) and a mean total uncertainty equal to 18.4%. Figure ~~12~~ 7 shows the mean IASI a priori profile and mean averaging kernels in the 6-16km partial column for the 39 comparison pairs. In the following, LIO3T measurements are smoothed according to these characteristics of the IASI retrievals.

Figures ~~13~~ 9 shows the comparison of the IASI and LIO3T partial columns time series. We obtain a good agreement between the datasets considering the uncertainties. We find a *D* of 11.3% between datasets (LIO3T ~~high~~higher than IASI). These results are in agreement with the 5-15% O_3 abundance difference of IASI in the troposphere compared to ECC soundings reported recently by Boynard et al. (2016). Note that~~the biomass burning seasonal cycle is clearly visible on the time series of both instruments in this partial column~~, due to the sparse comparison points, the southern hemisphere biomass burning season is barely visible on this plot.

5 Dataset and ~~time series~~climatologies

~~The Maïdo Observatory lidars (LIO3T, LIO3S, LI1200 and Doppler wind lidars)are operated on a routine basis two nights a week and intensively several times a year in campaign mode. Five campaigns were carried out during this 3 year-period: MALICCA (MAïdo LIdar Calibration CAmpaign) 1 (April 2013) and MALICCA 2 (November 2013) (Keckhut et al., 2015), LIDEOLE (LIDar EOLE)1 (November 2014) and LIDEOLE 2 (September 2015) - dedicated to the Doppler wind lidar intercomparisons with wind soundings - and MORGANE in May-July 2015 (Portafaix et al., 2015; Vérèmes et al., 2015; Duflot et al., 2016a; Posny et al., 2016).~~ Figure ~~14 shows the number of profiles (and hours of acquisition) per year; one can see that there are increasing numbers of profiles acquired each year, reaching a total of 84~~ 10 shows the monthly distribution of the number of O_3 profiles acquired by the NDACC/SHADOZ ECC (Gillot, 1998-2015, 568 profiles), LIO3T~~O_3 profiles for~~

the entire period . This increase is even more noticeable when looking at cumulative acquisition durations: from 28 hours in 2013 to 144 hours in 2015. This striking increase is $_{UR}$ (Université de la Réunion, 1998-2010, 427 profiles), and LIO3T (Maïdo Observatory, 2013-2015, 84 profiles). The low number of lidar profiles in the austral summer period (especially December-January) is explained by the system failures that occurred in 2013 and 2014 (KDP crystal and laser failures in September-November 2013, and Raman cell optics issues in May-July 2014), and by the huge effort made during the MORGANE campaign in 2015 to operate the high occurrence of cloudy skies. Especially, one can see that only one LIO3T system. Indeed, one of the main goals of this last campaign was the validation of profile is available for December (which ends up at 10km due to a misalignment of the LIO3TO_3 against ECC soundings in view of the application of the lidar to a NDACC labellisation.

Figure 15 shows the cross histogram of the lower and upper limits of the LIO3T O_3 profiles validity domain). Lower limit ranges of LIO3T profiles range from 6 to 10 km amsl10km, and upper limit from 12 to 19 km amsl. One can see that most 19km. Most LIO3T profiles start at 6 km 6km and end at 17-18 km amsl17-18km.

Figure 16 shows the seasonal distribution of the measured ozone profiles. Note that nearly half of March-April-May (MAM) profiles were acquired during the MORGANE campaign (light blue bar in Figure 16). Note also the few number of profiles in December-January-February (DJF) each year caused by the high cloudy skies occurrence frequency in the rainy season.

Figure 4 (bottom panel) shows the monthly averaged LIO3T O_3 profiles time serie. The same features as for the LIO3T$_{UR}$ and ECC climatologiescan be noticed (cf. Section 2.2)11 shows the three resulting monthly tropospheric O_3 climatologies, on which the following seasonal features can be observed:

- ozone abundance increase during the southern hemisphere biomass burning season (June-December peaking in October at a clear increase of O_3 abundance over the whole tropospheric column - especially between 2 and 10 km - starting in June and ending in December with a maximum in October of ≈ 9x1010x10^{11} molec/cm^3 on average between 6 4 and 10 kmamsl) ; ; this increase is due to the influence of air masses coming from South America, Southern Africa and South-East Asia (Edwards et al., 2006; Duflot et al., 2010) where the biomass burning season occurs every year during this period; O_3 abundance then presents a slow decay over the entire tropospheric column from January to May;

- ozonopause altitude decrease the decrease of the ozonopause altitude from ≈ 17km 17 km in December-July down to ≈ 15km amsl in late austral winter-spring.15 km in August-November (Sivakumar et al., 2011b), which is likely a combination of the spring and summer maximum of occurrence of stratosphere-to-troposphere exchanges (STE) above Reunion Island (Clain et al., 2010) and of the winter time thermal effect on the troposphere thickness;

Looking at the three climatologies, an additional seasonal pattern clearly appears: the minimum of ozone - the minimum of O_3 abundance in February between 10 and 16 km amsl (≈ 3x10^{11} molec/cm^3 on average), which is likely a signature of the austral summer deep convection bringing boundary layer-ozone layer-O_3 poor air masses up to the mid-upper troposphere.

In conclusion, the three datasets show a remarkable - and reassuring - agreement in terms of patterns and values.

Figure 17 12 shows the seasonal profiles derived from the LIO3T O_3 measurements. The southern hemisphere biomass burning season is still clearly visible in the September-October-November profile (SON), with an increase that covers the whole probed column, and also on the June-July-August (JJA) profile from 6 to 13 kmamsl.

6 Conclusions and future plans

A DIAL tropospheric ~~ozone lidar was installed and operated~~ O_3 lidar was operating on the Université de la Réunion campus site from 1998 to ~~2010. It provided~~ 2010, providing 427 ~~ozone profilesover the 13 years of operation~~O_3 profiles. In 2012, the system was moved up to the Maïdo Observatory and routine O_3 observations started in February 2013 by the LIO3T~~system~~. From then until January 2016, 84 O_3 profiles were acquired and LIO3T operation is ongoing. These O_3 measurements ~~was~~ were recently affiliated in the NDACC~~family~~.

The LIO3T ~~O_3~~ observation scheme is based on the DIAL technique, which currently detects two wavelengths, 289 and 316 nm, with multiple receivers. The transmitted wavelengths are generated by focusing the output of a quadrupled Nd:YAG laser beam (266 nm) into a ~~pair of Raman cells~~Raman cell, filled with high-pressure deuterium, using helium as buffer gas. With the knowledge of the ~~ozone~~ O_3 absorption coefficient at these two wavelengths, the range-resolved number density can be derived.

Optimal range for the actual system is 6-19km~~amsl~~, depending on the system performance and atmospheric conditions; for a 1-hour integration time, vertical resolution varies from 0.7 km at 6 km ~~amsl~~ to 1.3 km at 19 km~~amsl~~, and mean uncertainty over the 6-19km range is between $\approx$6 and $\approx$13%.

Comparisons with ancillary data were performed showing a good agreement between datasets considering the uncertainties: we found a ~~7.7~~6.8% *D* between LIO3T ~~O_3~~ observations and 8 ECC sondes simultaneously launched from the Maïdo Observatory (LIO3T ~~low), 10.3~~lower than ECC), 9.4% *D* between LIO3T ~~O_3~~ observations and 37 ECC sondes launched from the Gillot site during day time in a $\pm$ 24-hour window around lidar shooting (LIO3T ~~low~~lower than ECC), 11.8% *D* between LIO3T ~~O_3 and 11~~ and 12 ground-based NDACC FTIR measurements acquired during day time in a $\pm$ 24-hour window around lidar shooting in the 8.5-16 km partial colum (LIO3T ~~high~~higher than FTIR), and 11.3% *D* between LIO3T ~~O_3~~ and 39 simultaneous nighttime IASI observations over Reunion Island in the 6-16 km partial column (LIO3T ~~high~~higher than IASI).

ECC, LIO3T$_{UR}$ and LIO3T ~~O_3~~ monthly climatologies all exhibit the same range of values and the same seasonal patterns:

- the ~~ozone abundance increase~~ O_3 abundance increase between 6 and 10 km in austral winter and spring due to the southern hemisphere biomass burning season;

- the ozonopause altitude decrease from $\approx$ 17km to $\approx$ 15km from late austral winter to early austral summer due to the winter time thermal effect on the troposphere thickness combined to the enhanced occurrence of STE in austral spring and summer;

- the ~~ozone abundance minimum~~ O_3 abundance minimum between 10 and 16 km in late austral summer in the mid-upper troposphere due to deep convection uplifting ~~ozone-poor~~ O_3-poor air masses from the boundary layer.

~~This tropospheric ozone~~ The move of this lidar from the Université de la Réunion campus site up to the Maïdo observatory allows it to document the UT/LS region and to follow stratospheric and tropospheric intrusions with relevant vertical and time resolutions together with a reasonable uncertainty (1.5km, 20min and 10%, respectively, at 18km). This tropospheric O_3 data set covering the tropical free troposphere and ~~UTLS~~ UT/LS of a sparsely documented region (South Western Indian Ocean) constitutes an extremely valuable resource for the validation of satellite tropospheric ~~ozone~~ O_3 retrievals, analysis of the ~~ozone~~ O_3 variability and sources, dynamics analysis of case studies, and for long term atmospheric monitoring.

Future plans for the LIO3T ~~system are to~~are to: (1) use the available 532nm residual beam to detect and study aerosols in the free troposphere, TTL and lower stratosphere. The use of the infrared signal (1064nm) to study aerosols is also planned; (2) implement NDACC recommendations in the data processing (~~ozone~~ O_3 cross sections, background and saturation corrections uncertainties propagation, interfering gases); (3) calculate uncertainties due to the presence of aerosols in the troposphere using an iterative aerosol assessment procedure, ideally using the 532nm backscattered signal.

Acknowledgements. The authors acknowledge the European Communities, the Région Réunion, CNRS, and Université de la Réunion for their support and contribution in the construction phase of the research infrastructure OPAR (Observatoire de Physique de l'Atmosphère de La Réunion). OPAR is presently funded by CNRS (INSU) and Université de La Réunion, and managed by OSU-R (Observatoire des Sciences de l'Univers de La Réunion, UMS 3365). The authors also gratefully acknowledge E. Golubic, P. Hernandez and L. Mottet who are deeply involved in the routine lidar observations at the Maïdo facility. J. Witte (NASA/GSFC) is acknowledged for the ECC data reprocessing. IASI is a joint mission of EUMETSAT and the Centre National d'Etudes Spatiales (CNES, France). The IASI L1C data are distributed in near real time by EUMETSAT through the EUMETCast system distribution. The authors acknowledge the Aeris data infrastructure for providing access to the IASI L1C data and L2 temperature data used in this study. This work was undertaken in the framework of the EUMETSAT O_3M-SAF project (http://o3msaf.fmi.fi), the European Space Agency O_3 Climate Change Initiative (O_3-CCI, www.esa-ozone-cci.org). The ULB French scientists are grateful to CNES and Centre National de la Recherche Scientifique (CNRS) for financial support. PFC is grateful to Belspo and ESA (Prodex IASI.Flow project) for financial support. The colleagues from BIRA-IASB acknowledge the support from the Belgian Science Policy Office, as well as from ESA/PRODEX and the Copernicus programme (CAMS-VAL).

References

Ancellet, G., Mégie, G., Pelon, J., Capitini, R., and Renaut, D.: Lidar measurements of sulfur dioxide and ozone in the boundary layer during the 1983 Fos Berre Campaign, Atmos. Environ., 21, 2215-2226, 1987.

Baray, J.-L., Ancellet, G., Taupin, F. G., Bessafi, M., Baldy, S., and Keckhut, P.: Subtropical tropopause break as a possible stratospheric source of ozone in the tropical troposphere, J. Atmos. Solar-Terr. Phys. Vol. 60 , No. 1 , p. 27-36, 1998.

Baray, J.-L., Leveau, J., Porteneuve, J., Ancellet, G., Keckhut, P., Posny, F., and Baldy, S.: Description and evaluation of a tropospheric ozone lidar implemented on existing lidar in the southern tropics, App. Opt., Vol. 38, No. 33, 1999.

Baray, J. L., Leveau, J., Baldy, S., Jouzel, J., Keckhut, P., Bergametti, G., Ancellet, G., Bencherif, H., Cadet, B., Carleer, M., David, C., De Mazière, M., Faduilhe, D., Godin-Beekmann, S., Goloub, P., Goutail, F., Metzger, J. M., Morel, B., Pommereau, J.P., Porteneuve, J., Portafaix, T., Posny, F., Robert, L., and Van Roozendael, M.: An instrumented station for the survey of ozone and climate change in the southern tropics: Scientific motivation, technical description and future plans, J. Environm. Monit., 8, 1020-1028, doi:10.1039/b607762e, 2006.

Baray, J.-L., Courcoux, Y., Keckhut, P., Portafaix, T., Tulet, P., Cammas, J.-P., Hauchecorne, A., Godin Beekmann, S., De Mazière, M., Hermans, C., Desmet, F., Sellegri, K., Colomb, A., Ramonet, M., Sciare, J., Vuillemin, C., Hoareau, C., Dionisi, D., Duflot, V., Vérèmes, H., Porteneuve, J., Gabarrot, F., Gaudo, T., Metzger, J.-M., Payen, G., Leclair de Bellevue, J., Barthe, C., Posny, F., Ricaud, P., Abchiche, A., and Delmas, R.: Maïdo Observatory: a new high-altitude station facility at Reunion Island (21°S, 55°E) for long-term atmospheric remote sensing and in situ measurements, Atmos. Meas. Tech., 6, 2865-2877, doi:10.5194/amt-6-2865-2013, 2013.

Bass, A.M. and Paur, R.J.: The ultraviolet cross-sections of ozone: I: The measurements, II: Results and temperature dependence, Ozone Symposium, Greece, 1984.

Bègue et al., Long-range transport of volcanic aerosols plume over the Indian Ocean region during the Calbuco eruption, SSiRC Workshop, Potsdam, Poland, 2016.

Boynard, A., Hurtmans, D., Koukouli, M. E., Goutail, F., Bureau, J., Safieddine, S., Lerot, C. , Hadji-Lazaro, J. , Wespes, C., Pommereau, J.-P., Pazmino, A., Zyrichidou, I., Balis, D., Barbe, A., Mikhailenko, S. N., Loyola, D., Valks, P., Van Roozendael, M., Coheur, P.-F., and Clerbaux, C.: Seven years of IASI ozone retrievals from FORLI: validation with independent total column and vertical profile measurements, Atmos. Meas. Tech., 9, 4327-4353, 2016.

~~Brion, J., Chakir, A., Charbonnier, J., Daumont, D., Parisse, C., and Malicet, J.: Absorption Spectra Measurements for the Ozone Molecule in the 350-830 nm Region, J. Atmos. Chem., 30, 291-299, 10.1023/a:1006036924364, 1998.~~

Clain, G., J. L. Baray, R. Delmas, R. Diab, J. Leclair de Bellevue, P. Keckhut, F. Posny, J. M. Metzger, and J. P. Cammas, Tropospheric O_3 climatology at two Southern Hemisphere tropical/subtropical sites, (Reunion Island and Irene, South Africa) from ozonesondes, LIDAR, and in situ aircraft measurements, Atmos. Chem. Phys., 9, 1723-1734, 2009.

Clain, G., Baray, J.-L., Delmas, R., Keckhut, P., and Cammas, J.-P.: A Lagrangian approach to analyse the tropospheric ozone climatology in the tropics: Climatology of ~~stratosphere?troposphere~~ stratosphere-troposphere exchange at Reunion Island, Atmos. Environ., 44, 968-975, 2010.

Clerbaux, C., Boynard, A., Clarisse, L., George, M., Hadji-Lazaro, J., Herbin, H., Hurtmans, D., Pommier, M., Razavi, A., Turquety, S., Wespes, C., and Coheur, P.-F.: Monitoring of atmospheric composition using the thermal infrared IASI/MetOp sounder, Atmos. Chem. Phys., 9, 6041-6054, doi:10.5194/acp-9-6041-2009, 2009.

Daumont, D., Brion, J., Charbonnier, J., and Malicet, J.: Ozone UV Spectroscopy I: Absorption Cross-Sections at Room Temperature, J. Atmos Chem., 15, 145-155, 10.1007/bf00053756, 1992.

Dionisi,, D., Keckhut, P., Courcoux, Y., Hauchecorne, A., Porteneuve, J., Baray, J.-L., Leclair-de-Bellevue, J., Vérèmes, H., Gabarrot, F., Decoupes, R., and Cammas, J.-P.: Water vapor observations up to the lower stratosphere through the Raman lidar during the Maïdo LIdar Calibration Campaign, Atmos. Meas. Tech., 8, 1425-1445, 2015.

Donovan D. P., J. A. Whiteway, and A. I. Carswell: Correction for nonlinear photon-counting effects in lidar systems, Appl. Opt. 32, 6742-6753, 1993.

Duflot, V., Dils, B., Baray, J.-L., De Mazière, M., Attié, J.-L., Vanhaelewyn, G., Senten, C., Vigouroux, C., Clain, G., and Delmas, R.: Analysis of the origin of the distribution of CO in the subtropical southern Indian Ocean in 2007, J. Geophys. Res., 115, D22106, doi:10.1029/2010JD013994, 2010.

Duflot et al., Reunion Island NDACC Lidars Operations 2013-2016 and the MORGANE campaign, NDACC Lidar Working Group, Payerne, Switzerland, 2016a.

Duflot et al., Lidar UT/LS Observations at Reunion Island, WMO/SPARC/NDACC/GAW UT/LS Observations Workshop, Geneva, Switzerland, 2016b.

Edwards, D. P., et al., Satellite?observed Satellite-observed pollution from Southern Hemisphere biomass burning, J. Geophys. Res., 111, D14312, doi:10.1029/2005JD006655, 2006.

Gaudel, A., Ancellet, G., and Godin-Beekmann, S.: Analysis of 20 years of tropospheric ozone vertical profiles by lidar and ECC at Observatoire de Haute Provence (OHP) at 44°N, 6.7°E, Atmospheric Environment, doi:10.1016/j.atmosenv.2015.04.028, 2015.

Godin S. et al, Ozone differential absorption lidar algorithm intercomparison, Appl. Opt., 38, 6225-6236, 1999.

Hase, F., Blumenstock, T., and Paton-Walsh, C.: Analysis of the instrumental line shape of high-resolution Fourier transform IR spectrometers with gas cell measurements and new retrieval software, Appl. Opt., 38, 3417-3422, 1999.

Hinkley, E. D.: Laser monitoring of the atmosphere, Topics in applied physics, 14, Springer-Verlag, New York, 380 pp., 1976.

Hoareau, C., Keckhut, P., Baray, J.-L., Robert, L., Courcoux, Y., Porteneuve, J., Vömel, H., and Morel, B.: A Raman lidar at La Reunion (20.8°S, 55.5°E) for monitoring water vapour and cirrus distributions in the subtropical upper troposphere: preliminary analyses and description of a future system, Atmos. Meas. Tech., vol. 5, no. 6, pp. 1333-1348, 2012.

Hurtmans, D., Coheur, P.-F., Wespes, C., Clarisse, L., Scharf, O., Clerbaux, C., Hadji-Lazaro, J., George, M., and Turquety, S.: FORLI radiative transfer and retrieval code for IASI, J. Quant. Spectrosc. Ra., 113, 1391-1408, doi:10.1016/j.jqsrt.2012.02.036, 2012.

Johnson, B. J., S. J. Oltmans, H. Vömel, H. G. J. Smit, T. Deshler, and C. Kroeger, ECC Ozonesonde pump efficiency measurements and tests on the sensitivity to ozone of buffered and unbuffered ECC sensor cathode solutions, J. Geophys. Res., 107(D19), 4393, doi:10.1029/2001JD000557, 2002.

Johnson, B. J. et al., Sensor solutions for the ECC ozonesondes, WMO-GAW-SHADOZ-NDACC Ozone Sonde Experts Workshop, Edinburgh, Scotland, 2016.

Keckhut et al., Review of ozone and temperature lidar validations performed within the framework of the Network for the Detection of Stratospheric Change, J. Environ. Monit., 2004.

Keckhut, P., Courcoux, Y., Baray, J.-L., Porteneuve, J., Vérèmes, H., Hauchecorne, A., Dionisi, D., Posny, F., Cammas, J.-P., Payen, G., Gabarrot, F., Evan, S., Khaykin, S., Rüfenacht, R., Tschanz, B., Kämpfer, N., Ricaud, P., Abchiche, A., Leclair-de-Bellevue, J., and Duflot, V.: Introduction to the Maïdo Lidar Calibration Campaign dedicated to the validation of upper air meteorological parameters, J. Appl. Remote Sens, vol. 9, no. 1, 094099-094099, 2015.

Khaykin S., A. Hauchecorne, J. Porteneuve, J.-F. Mariscal, E. D'Almeida, J.-P. Cammas, G. Payen, S. Evan, P. Keckhut, Ground-based Rayleigh-Mie Doppler lidar for wind measurements in the middle atmospheres, ILRC 27, 10.1051/epjconf/201611913005, 2016.

Komhyr, W. D., Barnes, R. A., Brothers, G. B., Lathrop, J. A., and Opperman, D. P: Electrochemical concentration cell ozonesonde performance evaluation during STOIC 1989, J. Geophys. Res., 100, 9231-9244, 1995.

Lacis, A. A., Wuebbles, D. J., and Logan, J. A.: Radiative Forcing of Climate by Changes in the Vertical Distribution of Ozone, J. Geophys. Res., 95(D7), 9971-9981, 1990.

Leblanc at al.: Proposed standardized definitions for vertical resolution and uncertainty in the NDACC lidar ozone and temperature algorithms - Part 1: Vertical resolution, Atmos. Meas. Tech., 9, 4029-4049, doi:10.5194/amt-9-4029-2016, 2016a.

Leblanc at al,: Proposed standardized definitions for vertical resolution and uncertainty in the NDACC lidar ozone and temperature algorithms - Part 2: Ozone DIAL uncertainty budget, Atmos. Meas. Tech., 9, 4051-4078, doi:10.5194/amt-9-4051-2016, 2016b.

Leclair De Bellevue J., Réchou A., Baray J.-L., Ancellet G., and Diab R. D., Signatures of stratosphere to troposphere transport near deep convective events in the southern subtropics, J. Geophys. Res., VOL. 111, D24107, doi:10.1029/2005JD006947, 2006

Malicet, J., Daumont, D., Charbonnier, J., Parisse, C., Chakir, A., and Brion, J.: Ozone uv spectroscopy .2. Absorption cross-sections and temperature-dependence, J. Atmos Chem., 21, 263-273, 10.1007/bf00696758, 1995.

Martin, R. V., Jacob, D. J. , Yantosca, R. M., Chin, M., and Ginoux, P.: Global and regional decreases in tropospheric oxidants from photochemical effects of aerosols, J. Geophys. Res., 108(D3), 4097, doi:10.1029/2002JD002622, 2003.

McGee, T. J., Gross, M., Ferrare, R., Heaps, W., and Singh, U.: Raman dial measurements of stratospheric ozone in the presence of volcanic aerosols, Geophys. Res. Lett., 20, 955-958, doi:10.1029/93GL00751, 1993.

Mégie, G. J., Ancellet, G., and Pelon, J.: Lidar measurements of ozone vertical profiles, Appl. Opt., 24, 3454-3463, 1985.

Molina L. T. and Molina M. J., Absolute absorption cross sections of ozone in the 185 to 350nm wavelength range, J. Geophys. Res. 91, 14, 501-14, 508, 1986.

Morel et al., Evidence of tidal perturbations in the middle atmosphere over Southern Tropics as deduced from LIDAR data analyses, J. of Atmos. and Solar-Terrestrial Phys., 2002.

Pelon, J. and Mégie, G.: Ozone monitoring in the troposphere and lower stratosphere: Evaluation and operation of a groundbased lidar station, J. Geophys. Res.-Ocean., 87, 4947-4955,doi:10.1029/JC087iC07p04947, 1982.

Pelon J., Distribution verticale de l'ozone dans la troposphère et la stratosphère: étude expérimentale par télédétection laser et application aux échanges troposphère-stratosphère, Thèse de l'Université Paris 06, 1985.

Portafaix et al., Fine-scale study of a thick stratospheric ozone lamina at the edge of the southern subtropical barrier, J. Geophys. Res., 2003.

Portafaix T., S. Godin-Beekmann, G. Payen, M. de Mazière, B. Langerock, S. Fernandez, F. Posny, J.P. Cammas, J. M. Metzger, H. Bencherif, C. Vigouroux and N. Marquestaut, Ozone profiles obtained by DIAL technique at Maïdo Observatory in La Reunion Island: comparisons with ECC ozone-sondes, ground-based FTIR spectrometer and microwave radiometer measurements, ILRC 27, 10.1051/epjconf/201611905005, 2015.

Posny, F., Johnson, B. J., Metzger, J.-M., Duflot, V., Portafaix, T., Cullis, P., Thompson, A.M., Witte, J. C., La Reunion Island (21°S, 55.5 °E) SHADOZ/NDACC station: First re-processed ozonesonde data and comparisons with lidar measurements at the Maïdo Observatory, Quadriennal Ozone Symposium of the International Ozone Commission, QOS2016-192, 2016.

Rodgers C., Inverse Methods for Atmospheric Sounding: Theory and Practice, Series on Atmospheric, Oceanic and Planetary Physics, vol. 2, World Sci., Singapore, 2000.

Rodgers, C. D. and Connor, B. J.: Intercomparison of remote sounding instruments, J. Geophys. Res., 108, 4116, doi:10.1029/2002JD002299, 2003.

Savitzky A. and Golay M. J. E., Smoothing and Differentiation of Data by Simplified Least Squares Procedures, Anal. Chem., 1964, 36 (8), pp 1627-1639, DOI: 10.1021/ac60214a047, Publication Date: July 1964

Sivakumar et al., Rayleigh LIDAR and satellite (HALOE, SABER, CHAMP and COSMIC) measurements of stratosphere-mesosphere temperature over a southern sub-tropical site, Reunion (20.8°S; 55.5°E): climatology and comparison study, Ann. Geophys., 2011a.

Sivakumar V., Bencherif H., Bègue N., Thompson A. N., Tropopause Characteristics and Variability from 11 yr of SHADOZ Observations in the Southern Tropics and Subtropics, J. App. Met. Clim., 2011b.

Smit et al., Assessment of the performance of ECC-ozonesondes under quasi-flight conditions in the environmental simulation chamber: Insights from the Juelich Ozone Sonde Intercomparison Experiment (JOSIE), J. Geophys. Res., 2007.

Smit, H. G. J., and the Panel for the Assessment of Standard Operating Procedures for Ozonesondes (ASOPOS), Guidelines for homogenization of ozonesonde data, SI2N/O3S-DQA activity as part of "Past changes in the vertical distribution of ozone assessment", available at: http://www-das.uwyo.edu/%7Edeshler/NDACC_O3Sondes/O3s_DQA/O3S-DQA-Guidelines%20Homogenization-V2-19November2012.pdf, 2012.

Smit et al., Ozone Data Quality Assessment (O3S-DQA): Resolving inhomogeneities in long-term ozone sounding records and assessing their uncertainties, Quadriennal Ozone Symposium of the International Ozone Commission, QOS2016-246, 2016.

Stevenson, D. S, Dentener, F. J., Schultz, M. G., Ellingsen, K., van Noije, T. P. C., Wild, O., Zeng, G., Amann, M., Atherton, C. S., Bell, N., Bergmann, D. J., Bey, I., Butler, T., Cofala, J., Collins, W. J., Derwent, R. G., Doherty, R. M., Drevet, J., Eskes, H. J., Fiore, A. M., Gauss, M., Hauglustaine, D. A., Horowitz, L. W., Isaksen, I. S. A., Krol, M. C., Lamarque, J.-F., Lawrence, M. G., Montanaro, V., Müller, J.-F., Pitari, G., Prather, M. J., Pyle, J. A., Rast, S., Rodriguez, J. M., Sanderson, M. G., Savage, N. H., Shindell, D. T., Strahan, S. E., Sudo, K., and Szopa, S.: Multimodel ensemble simulations of presentday and near-future tropospheric ozone, J. Geophys. Res., 111, D08301, doi:10.1029/2005JD006338, 2006.

Sullivan, J. T., McGee, T. J., DeYoung, R., Twigg, L. W., Sumnicht, G. K., Pliutau, D., Knepp, T., and Carrion, W.: Results from the NASA GSFC and LaRC Ozone Lidar Intercomparison: New Mobile Tools for Atmospheric Research, Journal of Atmospheric and Oceanic Technology, 10.1175/JTECH-D-14-00193.1, 2015.

Thompson, A. M., Balashov, N. V., Witte, J. C., Coetzee, J. G. R., Thouret, V., and Posny, F.: Tropospheric ozone increases over the southern Africa region: bellwether for rapid growth in Southern Hemisphere pollution?, Atmos. Chem. Phys., 14, 9855-9869, 2014.

Uchino O., T. Sakai, T. Nagai, I. Morino, T. Maki, M. Deushi, K. Shibata, M. Kajino, T. Kawasaki, T. Akaho, S. Takubo, H. Okumura, K. Arai, M. Nakazato, T. Matsunaga, T. Yokota, S. Kawakami, K. Kita, and Y. Sasano, DIAL measurement of lower tropospheric ozone over Saga (33.24°N, 130.29°E), Japan, and comparison with a chemistry-climate model, Atmos. Meas. Tech., 7, 1385-1394, 2014.

Vérèmes et al., Water vapor profiles up to the UT/LS from Raman lidar at Reunion Island (21°S, 55°E) : technical description, data processing and comparisons with sondes, ILRC 27, New York, United States EDP Sciences, 119, pp.05004, ~~2016.~~ 2015.

Vérèmes et al., Multiple subtropical stratospheric instrusions over Reunion Island: observational, eulerian and lagrangian numerical modeling approaches, J. Geophys. Res., doi: 10.1002/2016JD025330, 2016.

Vérèmes H., G. Payen,,P. Keckhut, V. Duflot, J.-L. Baray, J.-P. Cammas, J. Leclair de Bellevue, S. Evan, F. Posny, F. Gabarrot, J.-M. Metzger, N. Marquestaut, S. Meier, H. Vömel, and R. Dirksen, A Raman lidar at Maïdo Observatory (Reunion Island) to measure water vapor in the troposphere and lower stratosphere: calibration and validation, Atmos. Meas. Tech. Discuss., doi:10.5194/amt-2017-32, 2017.

Vigouroux, C., De Mazière, M., Demoulin, P., Servais, C., Hase, F., Blumenstock, T., Kramer, I., Schneider, M., Mellqvist, J., Strandberg, A., Velazco, V., Notholt, J., Sussmann, R., Stremme, W., Rockmann, A., Gardiner, T., Coleman, M., and Woods, P.: Evaluation of tropospheric and stratospheric ozone trends over Western Europe from ground-based FTIR network observations, Atmos. Chem. Phys., 8, 6865-6886, 2008.

Witte Jacquelyn C., Anne M. Thompson, Herman G. J. Smit, Masatomo Fujiwara, Françoise Posny, Gert J. R. Coetzee, Edward T. Northam, Bryan J. Johnson, Chance W. Sterling, Maznorizan Mohammed, Shin-Ya Ogino, Allen Jordan, Zamuna Zainel, and Francisco R. da Silva, First reprocessing of Southern Hemisphere ADditional OZonesondes (SHADOZ) profile records (1998-2015) 1: Methodology and evaluation, J. Geophys. Res., in review.

Zhou, M., Vigouroux, C., Langerock, B., Wang, P., Dutton, G., Hermans, C., Kumps, N., Metzger, J.-M., Toon, G., and De Mazière, M.: CFC-11, CFC-12 and HCFC-22 ground-based remote sensing FTIR measurements at Reunion Island and comparisons with MIPAS/ENVISAT data, Atmos. Meas. Tech. Discuss., doi:10.5194/amt-2016-235, in review for Atmos. Meas. Tech., 2016.

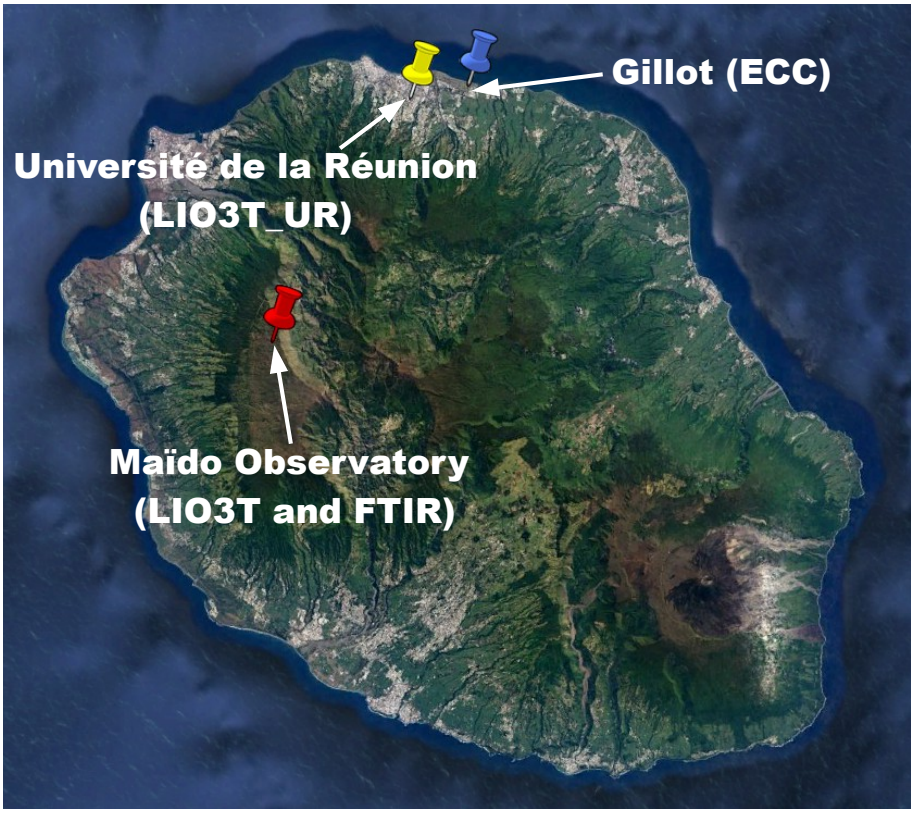

Figure 1. Map showing the locations of the different measurement sites ~~,~~ (Maïdo Observatory, Gillot, and University in Reunion Island) and instruments (LIO3T$_{UR}$, ECC, FTIR and LIO3T) used in this study.

~~Mean LIO3T$_{UR}$ uncertainty (black curve) and resolution (blue curve) at Université de la R'eunion.~~

~~Number of LIO3T$_{UR}$ ozone profiles per year.~~

~~Top left panel: Monthly ECC climatology (2005-2015, Gillot site) between 0 and 19km amsl; Top right panel: Monthly LIO3T$_{UR}$ climatology (1998-2010, Université de la Réunion campus site); Bottom panel: Monthly LIO3T climatology (2013-2015, Maïdo Observatory).~~

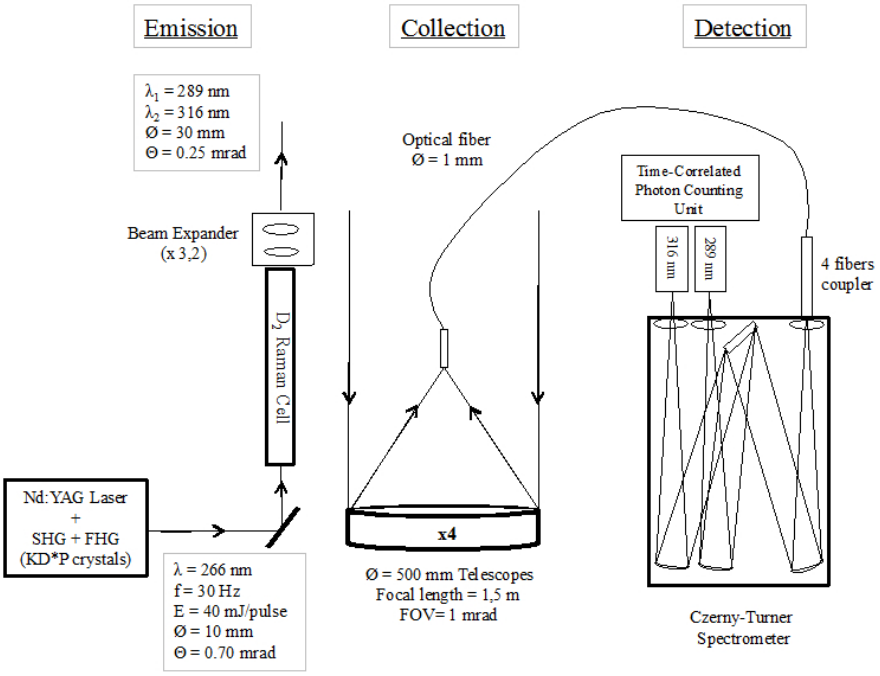

Figure 2. LIO3T ~~O_3 DIAL Experimental schematic~~instrumental schema.

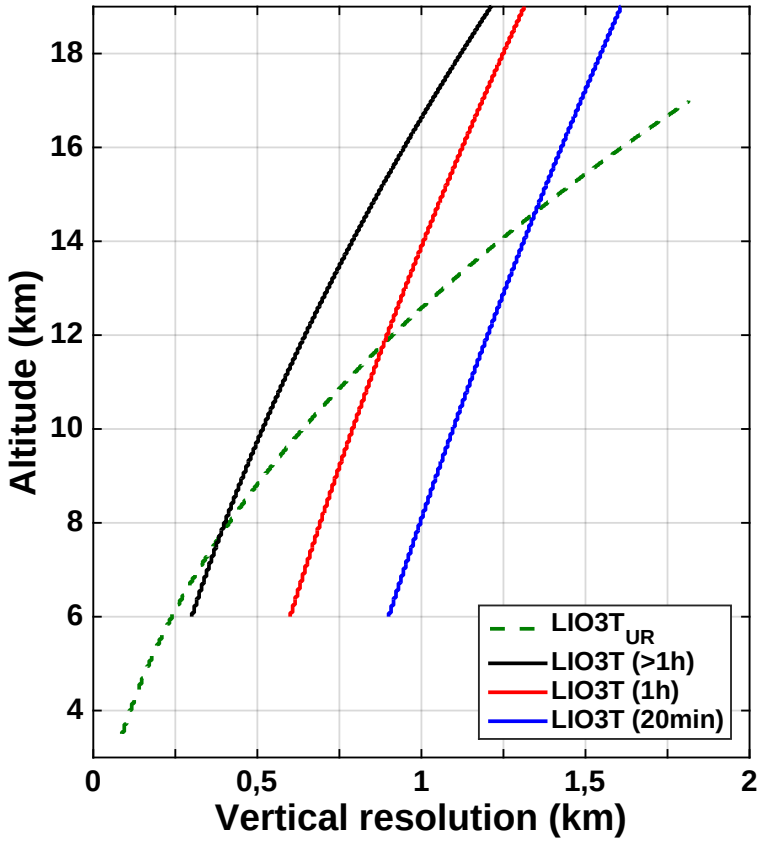

Figure 3. ~~Lower X-axis: ozone profile obtained on the 2013/07/09 for a 20 minutes~~ Mean vertical resolution of LIO3T$_{UR}$ profiles (~~blue~~ dashed green curve) ~~,~~ and of LIO3T profiles for integration times greater than 1 hour (~~red curve) and 3 hours (~~black curve)~~integration time. Uncertainties for each profile are given by dotted curves. Upper X-axis: corresponding resolution profiles for a 20 minutes (blue line)~~, equal to 1 hour (red ~~line~~curve) and ~~3 hours~~ equal to 20 minutes (~~black line~~blue curve)~~integration time~~.

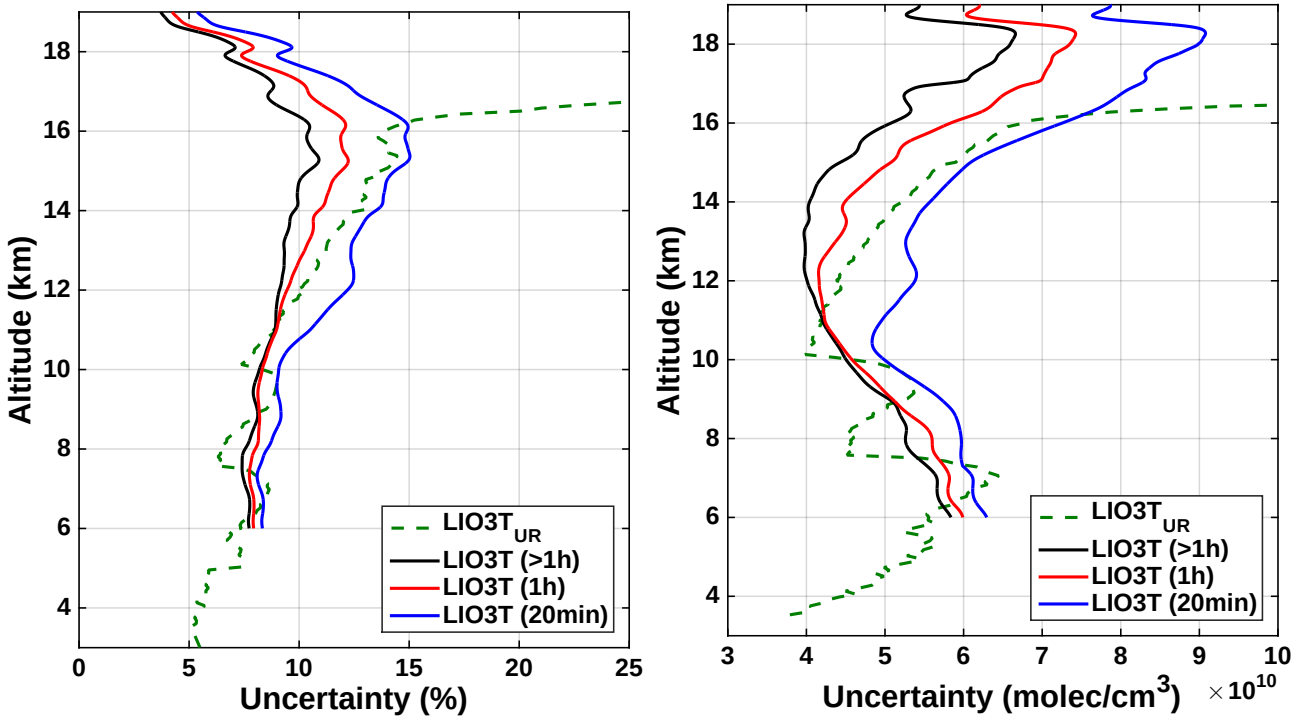

Figure 4. Mean uncertainties in % (left panel) and molec/cm^3 (right panel) of the LIO3T~~ozone~~ $_{UR}$ profiles (dashed green curve) and of the LIO3T profiles for integration times greater than 1 hour (black curve), equal to 1 hour (red curve) and equal to 20 minutes (blue curve).

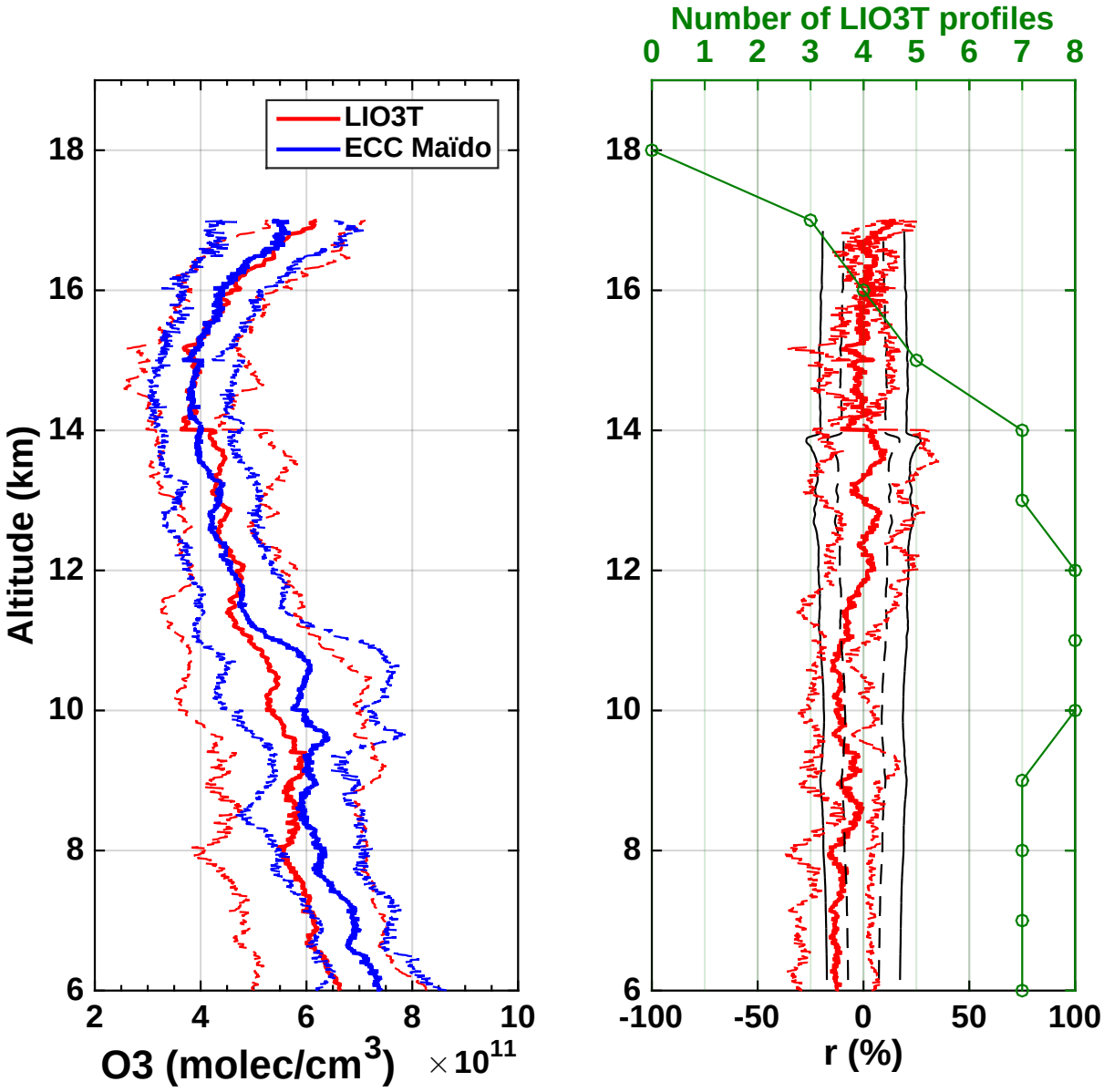

Figure 5. Left panel: mean LIO3T ~~ozone~~ O_3 profile (red curve) and mean ECC profile (blue curve) measured during the 8 intercomparison measurements performed at Maïdo. The ~~shaded areas~~ dashed lines give the 1 standard deviation around the mean; Right panel: mean ~~D~~ r between the LIO3T and ECC ~~mean~~ profiles (red curve), mean LIO3T uncertainty around zero (black dashed ~~curves~~lines) and mean LIO3T uncertainty + ECC accuracy around zero (black ~~curves and black shaded area~~lines). The red dashed lines give the 1 standard deviation around the r mean. The green line (upper X-axis) gives the number of LIO3T profiles used for comparison.

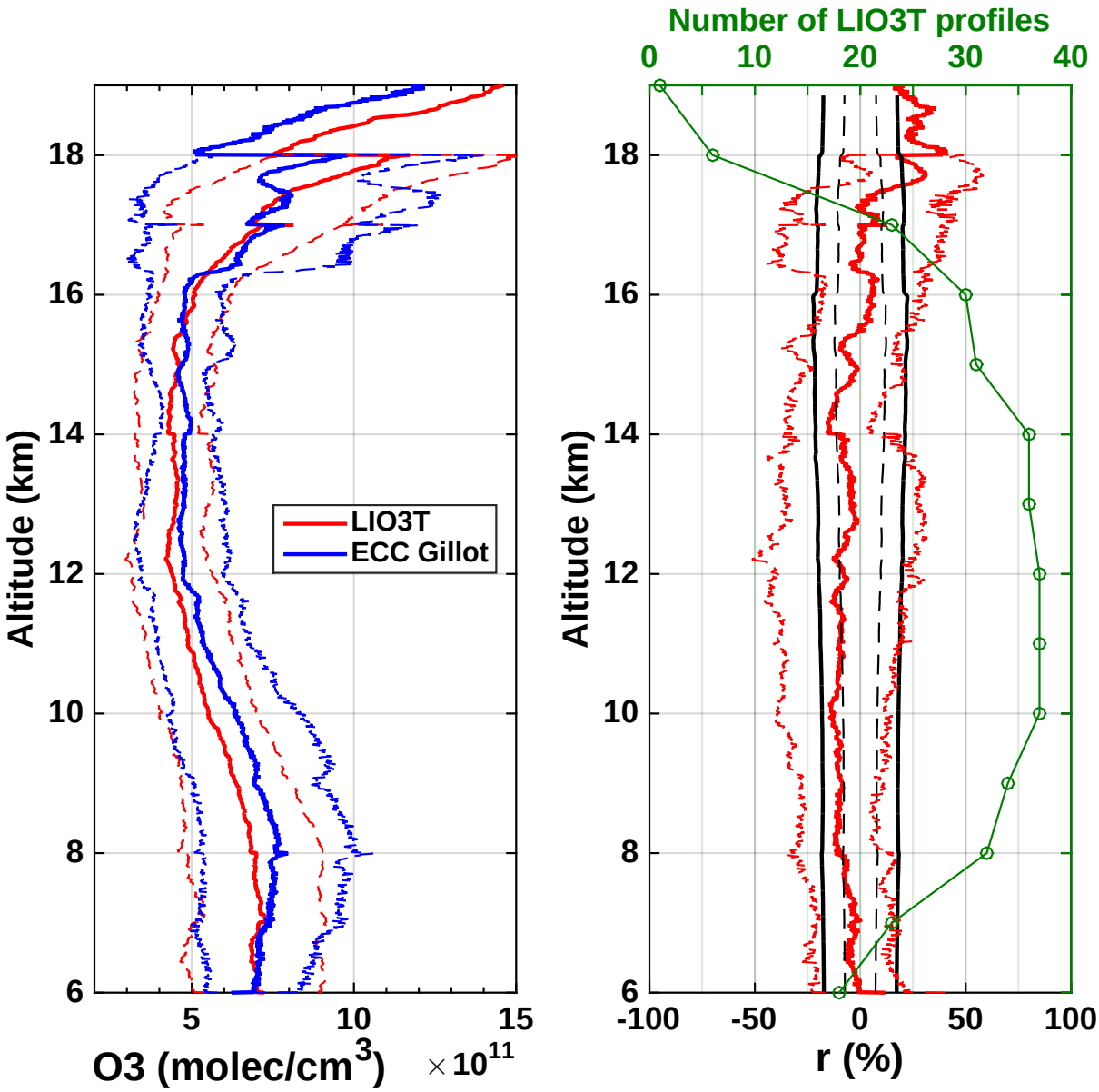

Figure 6. Same as ~~figure 8~~ Figure 5 for NDACC/SHADOZ Gillot ECC soundings and "full night" LIO3T profiles.

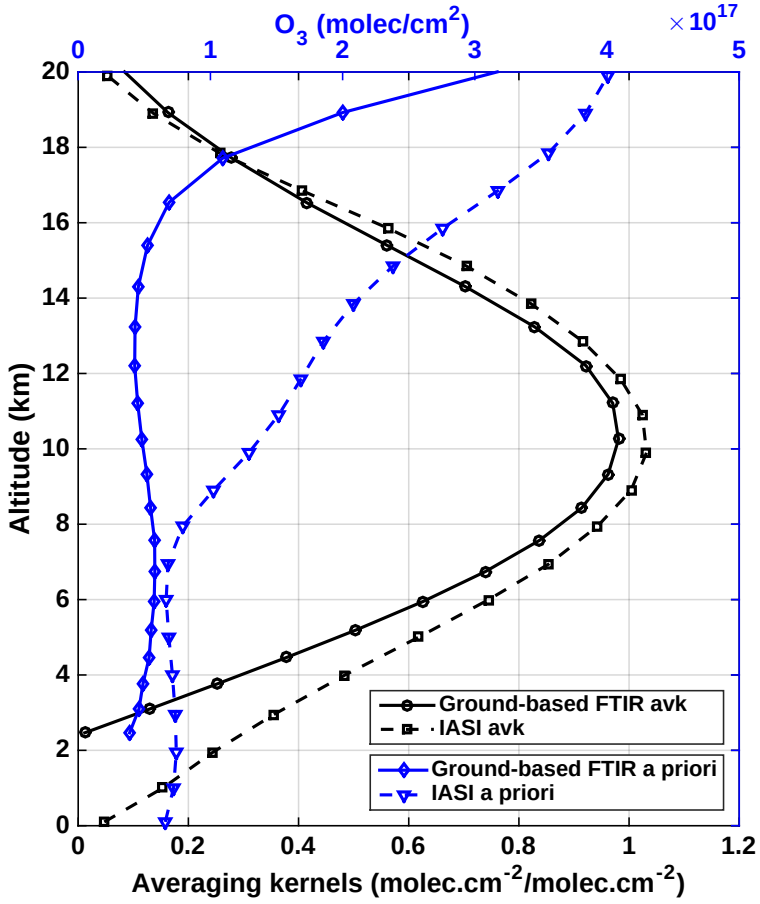

Figure 7. Lower X-axis: ground-based NDACC FTIR (black curve and circles) and IASI (black dashed curve and squares) averaging kernels for the 8-16 km ~~partial column (black curve~~ and ~~circles)~~6-16km partial columns, respectively; Upper X-axis: ground-based NDACC FTIR ~~ozone a priori profile~~ (blue curve and diamonds) and IASI (blue dashed curve and triangles) O_3 a priori profiles.

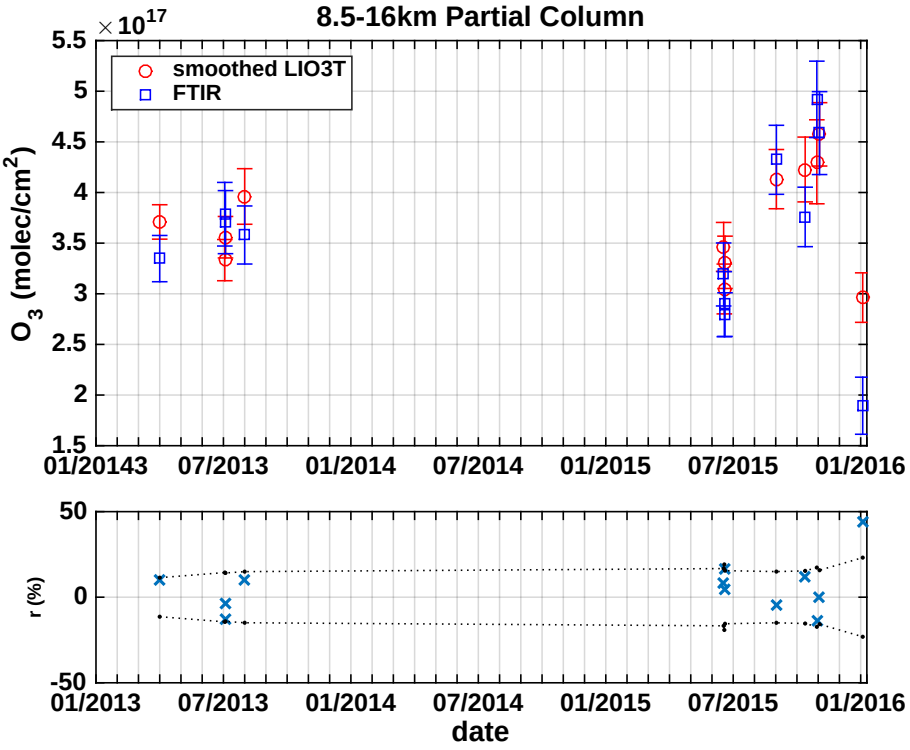

Figure 8. Upper panel: smoothed LIO3T (red circles) and ground-based NDACC FTIR (blue squares) 8.5-16km ~~ozone~~ O_3 partial columns. Vertical bars give uncertainties for each measurement; Lower panel: ~~relative difference~~ r (%) between LIO3T and FTIR measurements (blue crosses) superimposed on LIO3T + FTIR uncertainties around zero (black dotted lines and dots).

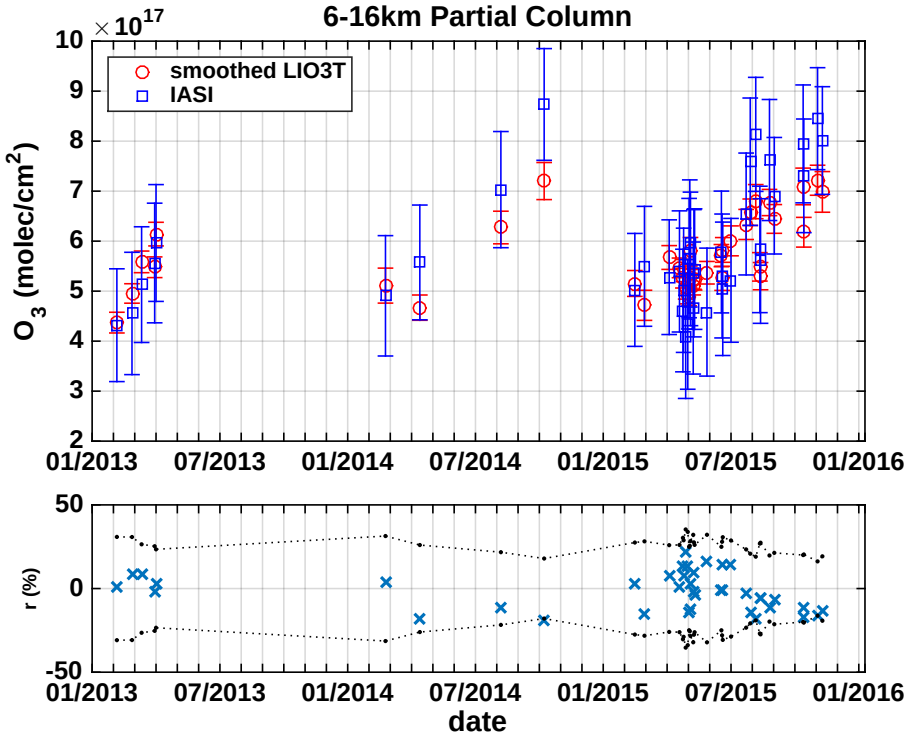

~~Upper~~ panel: smoothed LIO3T (red circles) and IASI (blue squares) 6-16km ~~ozone~~ O_3 partial columns. Vertical bars give uncertainties for each measurement; Lower panel: ~~relative difference~~ r (%) between LIO3T and IASI measurements (blue crosses) superimposed on LIO3T + IASI uncertainties around zero (black dotted lines and dots).

~~Upper~~ panel: smoothed LIO3T (red circles) and IASI (blue squares) 6-16km ~~ozone~~ O_3 partial columns. Vertical bars give uncertainties for each measurement; Lower panel: ~~relative difference~~ r (%) between LIO3T and IASI measurements (blue crosses) superimposed on LIO3T + IASI uncertainties around zero (black dotted lines and dots).

Figure 9. ~~Lower X-axis: IASI averaging kernels for the 6-16 km partial column (black curve and circles);~~ Upper ~~X-axis: IASI ozone a priori profile (blue curve and diamonds).~~

~~Upper~~ panel: smoothed LIO3T (red circles) and IASI (blue squares) 6-16km ~~ozone~~ O_3 partial columns. Vertical bars give uncertainties for each measurement; Lower panel: ~~relative difference~~ r (%) between LIO3T and IASI measurements (blue crosses) superimposed on LIO3T + IASI uncertainties around zero (black dotted lines and dots).

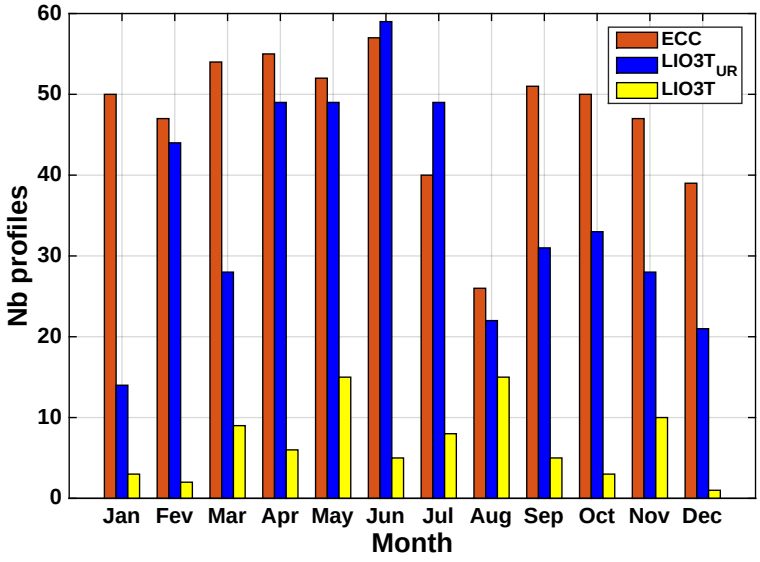

Figure 10. ~~Monthly distribution~~ Number of ~~the~~ O_3 profiles per month for ECC (1998-2015, 568 profiles), LIO3T$_{UR}$ (1998-2010, 427 profiles~~from~~) and LIO3T (January ~~2013 to January 2016. Annual total numbers of~~ 2013-January 2016, 84 profiles~~are given for each year together with cumulative acquisition durations~~).

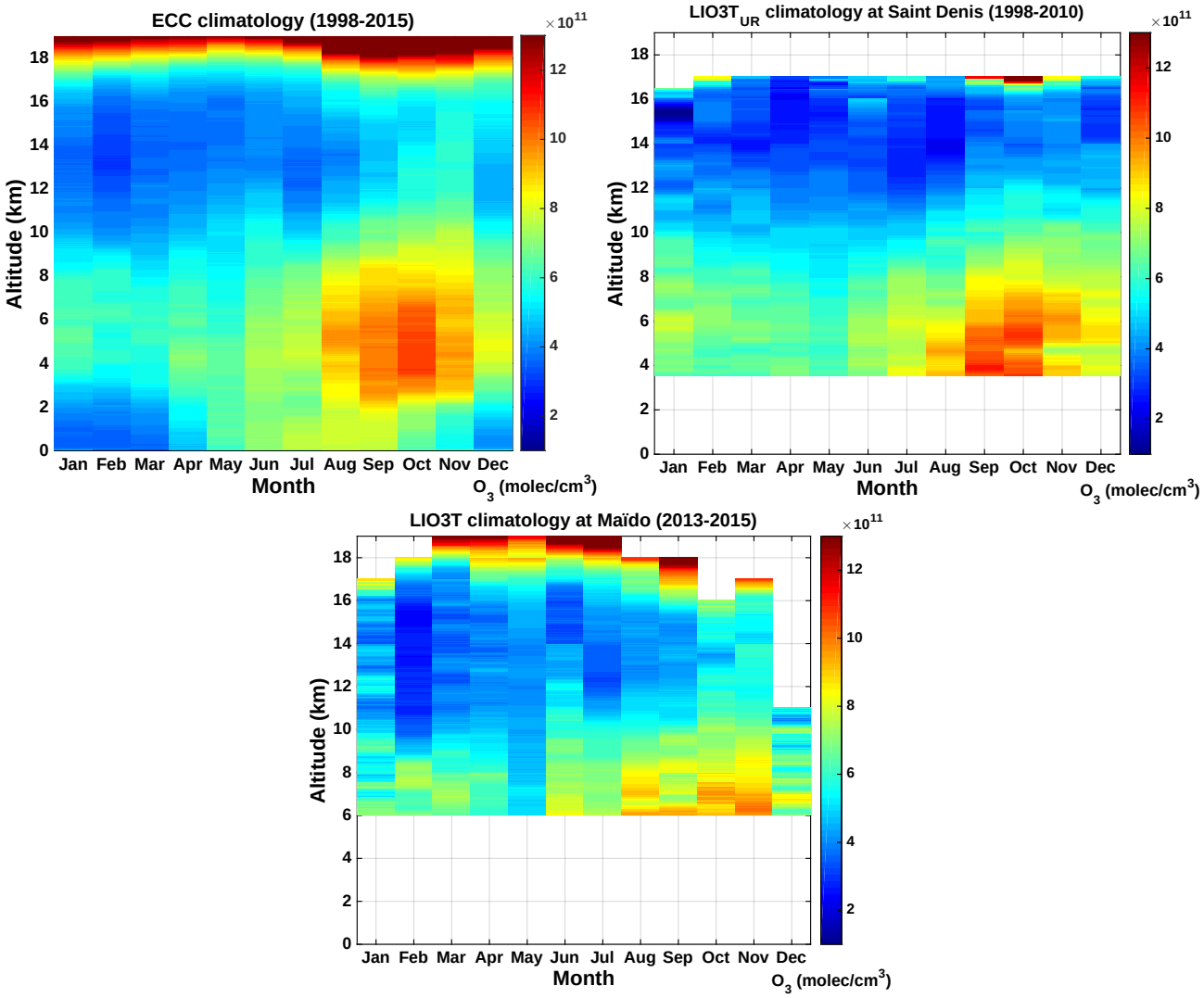

Figure 11. ~~Cross histogram of the lower~~ Monthly O_3 climatology between 0 and ~~upper limits of the LIO3T profiles validity domain~~ 19km derived from ECC sondes over 1998-2015 at Gillot site (~~relative occurrence in %~~Top left panel), ~~84 profiles~~from LIO3T$_{UR}$ over 1998-2010 at Université de la Réunion campus site (Top right panel) and from LIO3T over 2013-2015 at Maïdo Observatory (including data routinely performed and from intensive period of observations) (bottom panel).

~~Seasonal distribution of the ozone profiles measured by LIO3T for December-January-February (DJF), March-April-May (MAM), June-July-August (JJA) and September-October-November (SON). The light blue bar in MAM gives the number of ozone profiles acquired in May 2015 during the MORGANE campaign.~~

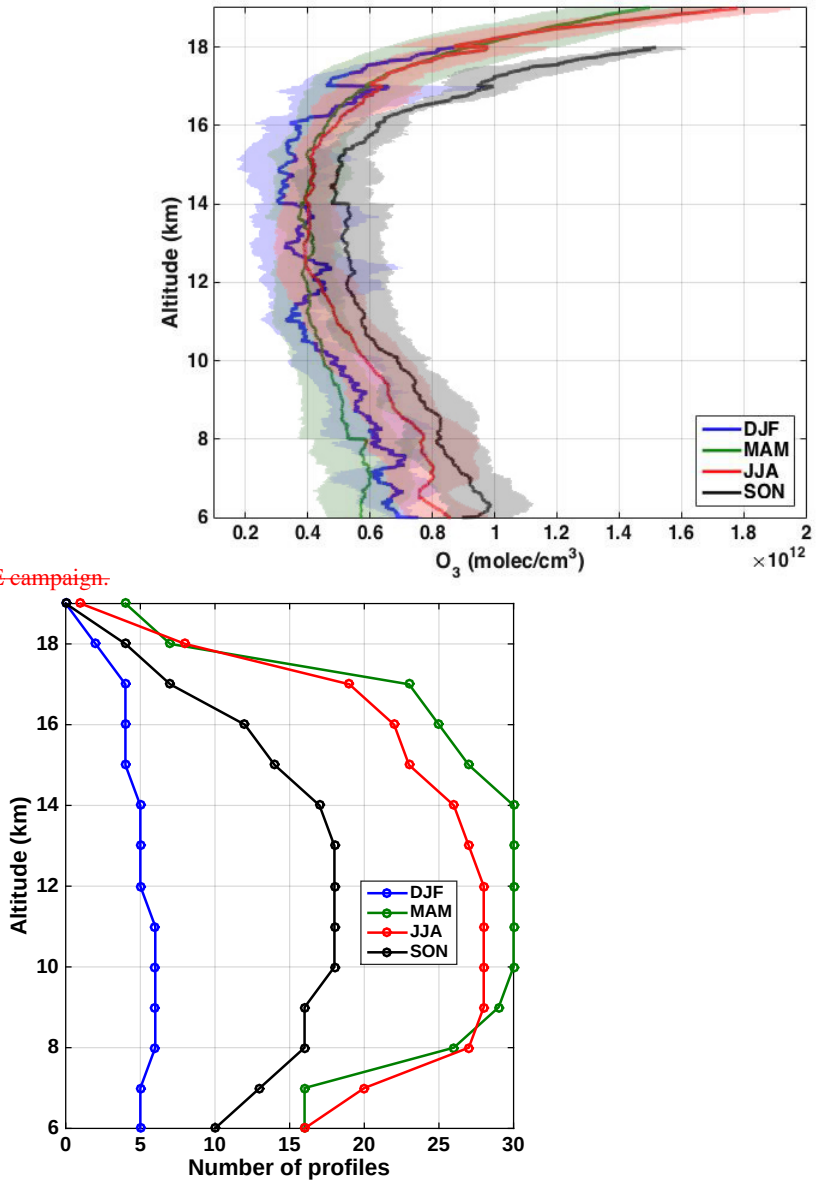

Figure 12. Left panel: Seasonal LIO3T O_3 profiles for DJF (blue curve - 8 profiles), MAM (green curve - 30 profiles), JJA (red curve - 25 profiles) and SON (black curve - 21 profiles). The shaded areas give the 1 standard deviation around the mean. Right panel: Number of LIO3T profiles used for each climatological profile.

~~Seasonal LIO3T ozone profiles for DJF (blue curve), MAM (green curve), JJA (red curve) and SON (black curve). The shaded areas give the 1 standard deviation around the mean.~~

Energy at 266 nm	Site	40 mJ/pulse Laser frequency Latitude	30 Hz Beam diameter Longitude	10 mm Raman cells length and diameter in/out Altitude (m)	1500mm and 20/55 mm Distance to Maïdo (km)
	Gases (pressure)in Raman cell Gillot	He (10 bar)and D (10 bar) ON/OFF wavelengths 20.893°S	289/316 nm 55.529 °E	9	26
	Emitted beam output diameter and divergence University	30mm and 0.25 mrad 20.902°S	55.485 °E	80	23
	Reception telescopes Maïdo Observatory	4 x 500 mm mosaic 21.079 °S	55.383 °E	2160	0

Table 1. Main LIO3T O_3 DIAL technical characteristicsCoordinates and distance to Maïdo Observatory of the observation sites used in this study.

Date	Profile valid range (km)
2013/06/24	6-14
2013/06/25	6-14
2015/05/11	6-17
2015/05/15	10-16
2015/05/26	6-12
2015/05/28	6-17
2015/07/06	6-15
2015/07/07	6-17

Table 2. Dates of comparisons with collocated ECC soundings and corresponding LIO3T O_3 profile valid ranges.